Influence of clay minerals and associated minerals in alkali activation of soils

Marsh, A. [a*], Heath, A. [a], Patureau, P. [b], Evernden, P. [a], Walker, P. [a]

[a] Department of Architecture & Civil Engineering, University of Bath, Bath, BA2 7AY, United Kingdom

[b] Department of Chemistry, University of Bath, Bath, BA2 7AY, United Kingdom

[*] corresponding author: a.marsh@bath.ac.uk

Abstract

Alkali activation is promising for low environmental impact soil stabilisation. Given soils' complexity, there is a lack of fundamental understanding of how the different components in soil influence their alkali activation behaviour. A novel method was developed to compare three natural soils with synthetic versions. Precursors and products were characterised by XRD, SEM, TGA and FTIR to explore the soils' alkali activation phase formation behaviour. It is shown that only the clay minerals will determine phase formation, whereas most associated minerals had negligible influence. The trade-off between Na:Al and NaOH concentration in mix design means lower plasticity soils are more suitable.

Graphical abstract

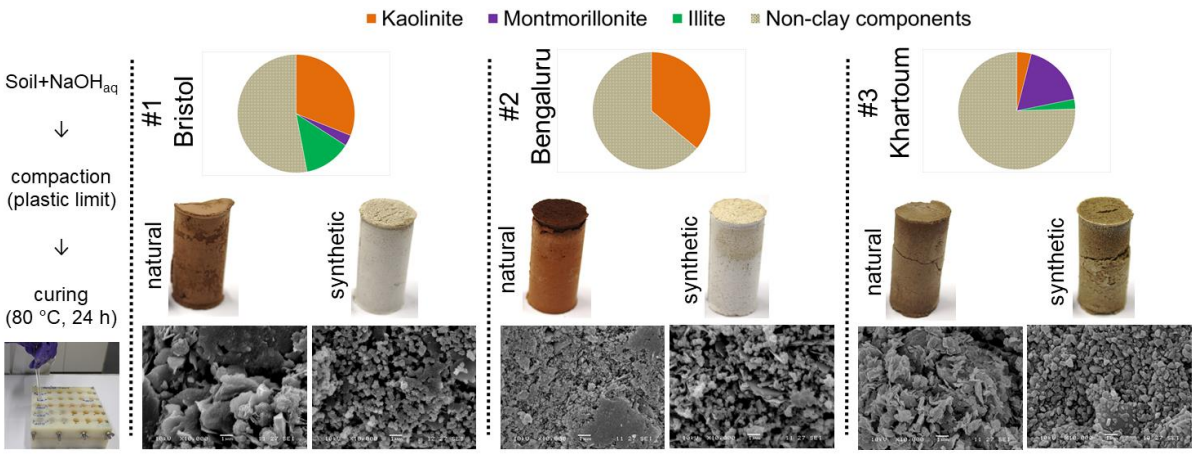

Keywords

Alkali activation; geopolymer; zeolite; soil; earth; stabilisation; clay mineral; associated minerals

Highlights

- Synthetic soils prepared to compare with natural soils
- Type and size of clay mineral influences type and size of products formed
- Iron compounds may have a retarding effect on geopolymer formation
- Composition trade-off between Na:Al molar ratio and NaOH solution concentration

1 Introduction

Alkali-activated materials are a growing area of interest in construction material development, due to their versatility in using a range of precursors and their potential for low environmental impact [1]. One application for alkali activation is soil stabilisation [2-4]. Research in this area has concentrated on the route of indirect alkali activation – the addition of reactive aluminosilicates to a soil, which are then transformed to form a stabilising phase. Additions have included fly ash [5], GGBS [6, 7], agricultural wastes [8-10], metakaolin [11, 12], volcanic ash [13] and others [2]. The alternative route of direct alkali activation - transforming the clay minerals in soil, without the addition of external aluminosilicates – has been less explored. This route has the possible benefits of being more versatile in areas where there is not a readily available source of reactive aluminosilicate, negating the troublesome effects of some clays in soil (e.g. swelling clays), and still retaining improvements in embodied carbon [14]. There is also a general benefit of developing methods to understand the alkali activation behaviour of lower purity aluminosilicates. This is to enable a wider range of precursors to be used, and hence greater impact of alkali-activated materials [15-17]. Previous research in direct alkali activation of clays and soils has mostly focussed either on relatively simple systems such as metakaolin [18] and kaolinite [19], with only a small number of studies on more complex natural soils [20-24]. The objectives of these studies have typically been to understand the effect of alkali activator and curing variables on the reaction, or simply the strength of the end products. This approach has been valuable in gaining an understanding of the fundamentals of the alkali activation process, as well as an empirical understanding of the range of these variables which typically give optimal results. However, in order to determine the feasibility of alkali-activated soils as a scalable technology, it is necessary to determine which compositional factors are important in making a given soil well-suited for activation, and which are not. This requires a more systematic approach to considering the influence of both the clay minerals in the reaction [25], and the influence of associated minerals in soils, some of which are known to be reactive in alkali activation. This has been done to some extent for common clay mineral deposits [26], but without isolating the effect of clay minerals other than kaolin.

The composition of sub-soils can be considered to consist of clay minerals, associated minerals (i.e. naturally occurring non-clay minerals) [27, 28] and some amount of organic compounds present in humic substances [29]. Soils with low organic content are used for stabilised soil materials, as this is a general requirement in earth building [30]. The composition of soils can vary greatly between different locations, as well as varying with depth in a single location [29]. The direct alkali activation behaviour of the common clay minerals is still being investigated, but a basic understanding of their behaviour as

individuals [25, 31] and in mixtures [32] has already been established under comparable processing conditions. In contrast, as a group, common associated minerals – especially in the context of soil systems - are less well understood.

The aim of this study is to investigate the relative influence of clay minerals and associated minerals in determining the direct alkali activation behaviour of soils. By using multi-component systems to close the gap between laboratory studies and real conditions, it is intended to gain a better understanding for a direct application in construction. This approach will improve our ability to predict which soils are suitable for alkali activation, rather than a trial and error approach of individually testing every different naturally occurring soil. This is the first known attempt to isolate the effect of associated minerals in soil on alkali activation using this approach.

2 Materials and Methods

2.1 Materials

Natural soils were used from: Bristol, U.K.; Bengaluru, India, and Khartoum, Sudan. Three soils were used to give a basic test of how consistent the findings were across different soil compositions. These particular soils were selected as they had previously been characterised [33, 34]. The particle size distribution (Figure 1) was measured by a combination of wet-sieving, to measure particle grading from 2 mm – 63 µm, and hydrometer testing, to measure particle grading <63 µm [35]. All three soils were fine-grained under the USCS terminology, with Bristol as a lean clay (CL) [33], Bengaluru as a lean clay (CL) and Khartoum as an intermediate clay (CI) [34]. Regarding colour, Bristol was brown, Bengaluru red and Khartoum brown-grey. Calcination is a common processing step in alkali activation of clay minerals, as it generally improves reactivity by the dehydroxylation of clay minerals - in particular, the conversion of kaolinite to metakaolin. In this study, it was chosen not to use calcination for two reasons. Firstly, because it increases the environmental impact of the precursor [36]. Secondly, because the ideal calcination temperature depends on the type and nature of clay minerals present [37], and in soils with different clay minerals choosing an optimal, single calcination temperature would be difficult.

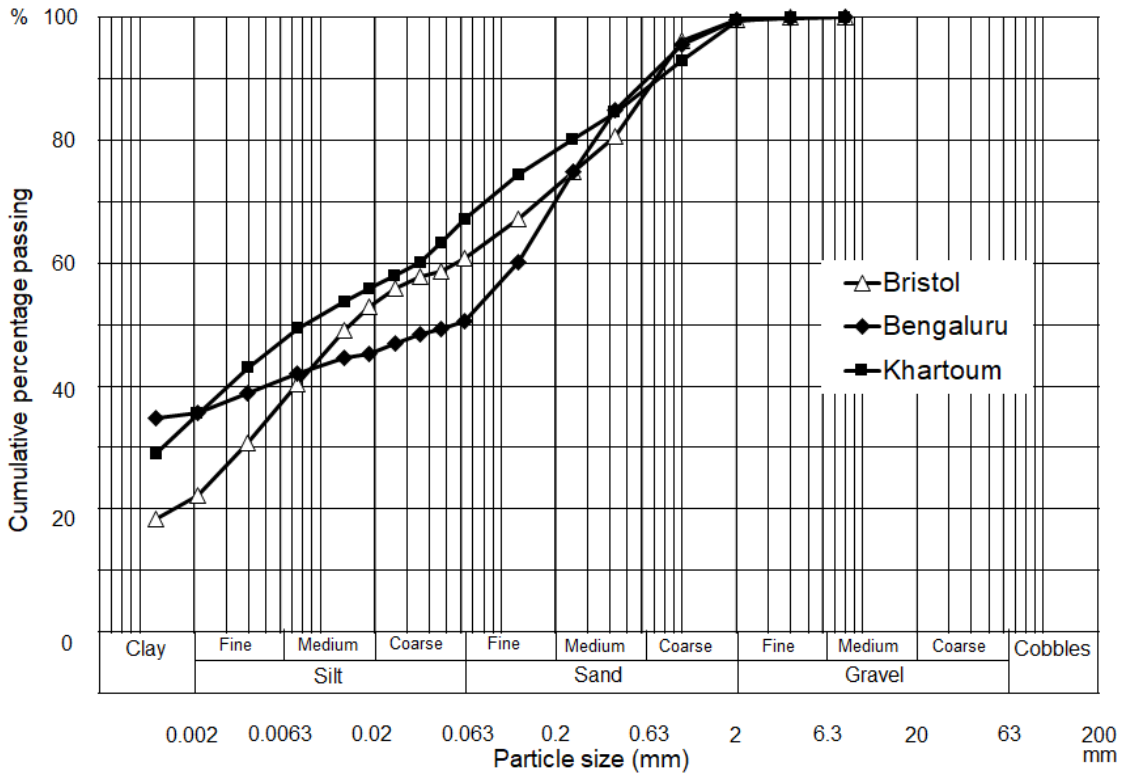

Figure 1: The particle size distribution of the three natural soils.

To manufacture synthetic soils, Imerys Speswhite kaolin (mined from Cornwall, U.K.), K10 montmorillonite (Sigma-Aldrich, product no. 69866-1KG) and Clay Minerals Society IMt-2 (Silver Hill) illite were used as precursor clays. Builders' fine quartz sand was used as an inert aggregate, sieved to <425 μm and washed clean with distilled water. This contained quartz, with a trace amount of calcite. Chemical compositions of the natural and synthetic soils were determined by energy dispersive X-rays (JEOL SEM6480LV with Oxford INCA X-Act SDD X-ray detector) at an accelerating voltage of 20 kV, a chamber pressure of 30 Pa, a Si wafer as a standard, and measuring ≥ 3 scan areas per sample. The soil powders were mounted on a sticky carbon tab on top of an aluminium stub, and were not coated. Specific surface area was measured using the BET method [38], using a Micromeritics 3-Flex. 2 g of each precursor powder were degassed ex-situ in a N_2 atmosphere under atmospheric pressure at 250°C for ≥ 70 h, and then degassed in-situ under vacuum at 250°C for 14 h.

The natural and synthetic soils' chemical compositions are given in Table 1. The natural and synthetic soils' specific surface areas are given in Table 2. In order to ensure consistency, the soils were ground by hand in isopropanol until they passed through a 425 μm sieve. The precursors were activated using sodium hydroxide pellets of >98% purity (Sigma-Aldrich, product no. 06203).

Table 1: Chemical composition of the natural (nat)and synthetic (syn) soils in oxide wt%.

Soil	Al_2O_3	CaO	CuO	Fe_2O_3	K_2O	MgO	MnO	Na_2O	SiO_2	SO_3	TiO_2	Total
Bristol-nat	22.85	1.29	0.34	9.75	4.84	1.16	0.00	0.25	57.76	0.39	1.37	100.00
Bengaluru-nat	24.05	0.38	0.08	12.10	1.21	0.26	0.00	0.00	60.73	0.08	1.11	100.00
Khartoum-nat	11.60	11.45	0.17	10.36	1.12	2.46	0.41	0.64	60.20	0.30	1.30	100.00
Bristol-syn	32.93	0.44	0.00	2.36	2.98	0.37	0.00	0.00	60.71	0.06	0.13	100.00
Bengaluru-syn	37.65	0.52	0.13	1.62	2.49	0.14	0.00	0.00	57.45	0.00	0.00	100.00
Khartoum-syn	16.63	0.50	0.00	3.93	2.09	1.00	0.00	0.00	75.28	0.00	0.57	100.00

Table 2: Specific surface areas of the natural (nat) and synthetic (syn) soils in oxide wt%.

Soil	Specific surface area (m^2g^{-1})
Bristol-nat	17.6
Bengaluru-nat	33.7
Khartoum-nat	36.9
Bristol-syn	14.0
Bengaluru-syn	6.7
Khartoum-syn	42.0

2.2 Synthesis procedure

The phase compositions in the natural Bristol [33] and Khartoum [34] soils had been previously quantified. The Bengaluru soil was found to contain kaolinite as the only clay mineral, the mass proportion of which was assumed to be the same as the clay fraction (<2 μm particle size). Using this information about the phase compositions of the natural soils (Table 3), synthetic soils were prepared. The compositions of the synthetic soils were determined in order to have the same types and proportions of clay minerals as each respective natural soil - but, instead of the associated minerals found in the natural soils, the remaining mass was made up with quartz sand as a filler. Using these proportions of clay minerals and quartz sand, the synthetic soils were prepared to have compositions given in Table 3. These were made by adding the constituent ingredients together in a beaker, then dry-mixing for 5 minutes with a magnetic stirrer (Stuart UC152 heat-stir). Their chemical compositions are given in Table 1.

*Table 3: Compositions of natural (nat) and synthetic (syn) soils used. *Natural associated minerals are assumed not to participate in the reaction.*

Sample	Kaolinite (%)	Montmorillonite (%)	Illite (%)	Natural associated minerals* (%)	Inert filler sand (%)
Bristol-nat	31	3	13	53	0
Bristol-syn	31	3	13	0	53
Bengaluru-nat	36	0	0	64	0
Bengaluru-syn	36	0	0	0	64
Khartoum-nat	4	18	3	75	0
Khartoum-syn	4	18	3	0	75

As previously described [31], the compositions in Table 4 were determined to provide samples of a predetermined Na:Al ratio (chosen to be 1), whilst maintaining the wet mix workability at the plastic limit. In order to be consistent about calculating the reactive moles of Al, a working assumption was made that only the clay minerals would react in alkali activation. Therefore, molar quantities of Al in each soil were calculated from the clay contents and generic structural formulae of the clay minerals. To model workability behaviour, Atterberg plastic limit measurements [39] were undertaken for each of the natural soils over a range of sodium hydroxide solution concentrations [35], shown in Figure 2. The behaviour matched well for the synthetic soils too.

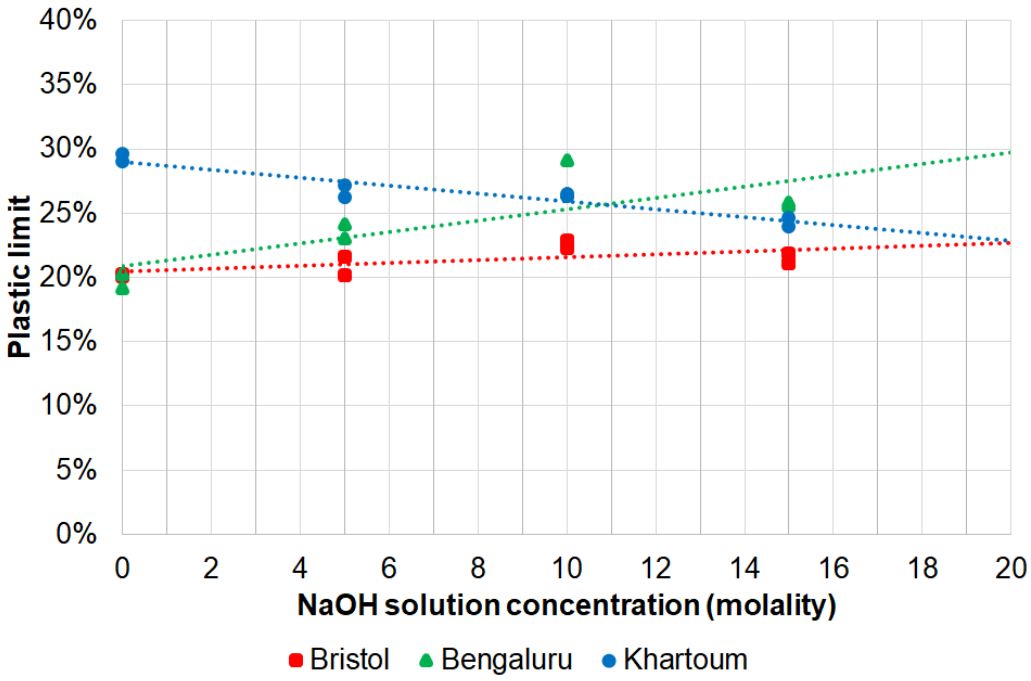

Figure 2: Variation in plastic limit with sodium hydroxide solution concentration for the three natural soils.

The soil samples were activated by adding an aqueous sodium hydroxide solution. Solutions of different concentrations were prepared by adding sodium hydroxide pellets to distilled water, mixing with a magnetic stirrer (Stuart UC152 heat-stir) for a minimum of 2 h until fully dissolved and then allowing to cool. Varying quantities of activating solutions were added to 20 g of each soil, as given in Table 4. Each mixture of activating solution and soil was mixed by hand for 3 minutes, providing a consistent and well-distributed mixture. The high viscosity of the samples allowed them to be compacted by hand into 18 mm x 36 mm cylindrical Teflon moulds by tamping with a glass rod in three layers for each sample, using 25 blows for each layer. Samples were cured in an air atmosphere in an 80 °C oven for 24 h in their moulds. After curing, activated samples in the Bristol and Bengaluru soil series were not fully dried so required further drying, by storing for 48 h in a vacuum dessicator. This phenomenon of slow drying has previously been observed in other alkali-activated clay-based systems [25]. After demoulding, samples were aged for 28 days in a controlled environment of 20 ± 0.5°C and 50 ± 2.5% relative humidity. An air atmosphere was intentionally used for both curing and ageing, to provide conditions representative of industrial brickmaking processes. A control sample was made for each composition, by adding distilled water and then mixing and curing in the same manner.

Due to the experimental constraints of plastic limit consistency and Na:Al = 1 (with the simplifying assumption made that Na available for reaction was supplied solely from the NaOH solution, and none from the soils), the NaOH solution was a lower concentration for Khartoum (4.1 M) than for the other soils (10.2 M and 13.2 M) (Table 4). Therefore, to test

whether the difference in behaviour was due to a lower concentration, activation of the Khartoum soils was repeated using a 10 M NaOH activating solution whilst maintaining the plastic limit condition, and hence giving an Na:Al molar ratio > 1. These results are included in an Appendix.

Table 4: Composition of activating solutions used for 20 g of dry soil, for the control (cont) and activated (act) samples.

Sample	Water (g)	NaOH (g)	[NaOH] (molarity)
Bristol-nat-cont	4.04	n/a	n/a
Bristol-nat-act	4.41	2.56	13.2
Bristol-syn-cont	4.04	n/a	n/a
Bristol-syn-act	4.41	2.56	13.2
Bengaluru-nat-cont	3.94	n/a	n/a
Bengaluru-nat-act	5.13	2.23	10.2
Bengaluru-syn-cont	3.94	n/a	n/a
Bengaluru-syn-act	5.13	2.23	10.2
Khartoum-nat-cont	5.86	n/a	n/a
Khartoum-nat-act	5.54	0.94	4.1
Khartoum-syn-cont	5.86	n/a	n/a
Khartoum-syn-act	5.54	0.94	4.1

2.3 Characterisation methods

The set of characterisations was performed at 28 ±2 days ageing time, and (with the exception of SEM imaging) was done using powders prepared from the cured samples. These were ground by hand, having been wetted with isopropanol to avoid damaging the clay minerals' crystal structures [40]. For XRD and TGA, powders were ground until there was no further discernible reduction in particle size, and so were comparable between samples. Any variation in particle size of the ground powders was not expected to have any noticeable effect on characterisation results. For FTIR, due to the constraints on particle size

when making measurements in reflection mode, and the wider particle size distribution in soils compared to clays, powders were ground until they passed through a 75 μm sieve.

Powder X-ray diffraction (XRD) analysis was performed to identify phases with a Bruker D8 Advance instrument using monochromatic CuKα1 L3 (λ = 1.540598 Å) X-radiation and a Vantec superspeed detector. A step size of 0.016 °(2θ) and step duration of 0.3 seconds were used. For finer scans of the < 2 μm size fraction of the natural soils, a step size of 0.0076 °(2θ) and step duration of 0.6 seconds were used. Powder samples were prepared using the pressed glass slide method. Patterns were corrected for sample height shift by calibrating to the most intense quartz reflection (101) at 26.6 °(2θ), and normalised to the most intense reflection in each respective pattern. Phase identification was done using Bruker EVA software, using reference patterns from the Joint Committee on Powder Diffraction Standards (JCPDS) database.

Fourier Transform Infrared Spectroscopy (FTIR) was done to characterise molecular bonding, using a Perkin-Elmer Frontier with a diamond Attenuated Total Reflectance (ATR) head. For FTIR, powder samples were ground further until they passed through a 75 μm sieve. Spectra were collected over a range of 4000 - 600 cm^{-1} using a resolution of 4 cm^{-1} and 5 scans per spectrum. Corrections were made for ATR and background using Perkin-Elmer Spectrum software. Spectra were normalised to the most intense band in each respective spectrum.

Scanning electron microscope (SEM) imaging was used to characterise phase size and morphology, using a JEOL SEM6480LV in secondary electron mode with an accelerating voltage (AV) of 10 kV. Unpolished samples were used to enable easier distinction of particle morphology in the microstructures, and also given the friability of some of the samples. Bulk specimens were sputter coated with gold for 3 minutes. All images were taken of regions in the bulk of the specimen, >2 mm away from the edge.

3 Results

3.1 Macroscopic behaviour

No unusual curing shrinkage or expansion defects were observed in any of the samples after curing (Figure 3), which have been previously observed in alkali activated clays [25]. The difference in colour between the natural and synthetic clays is mostly attributable to the presence of iron compounds, as reported in Table 1 [29]. Most of the soils did not undergo any changes of colour after activation. Exceptions included: the Bristol natural soil darkened slightly; the Khartoum synthetic soil turned a shade of brown, and both the Bengaluru real soil and the Bristol synthetic soil had a strip of darker material at the top (i.e. the open end of

the mould). This last phenomenon is likely to be associated with the one-dimensional flow of soluble matter to the top of the sample, since a mould with one open end was used.

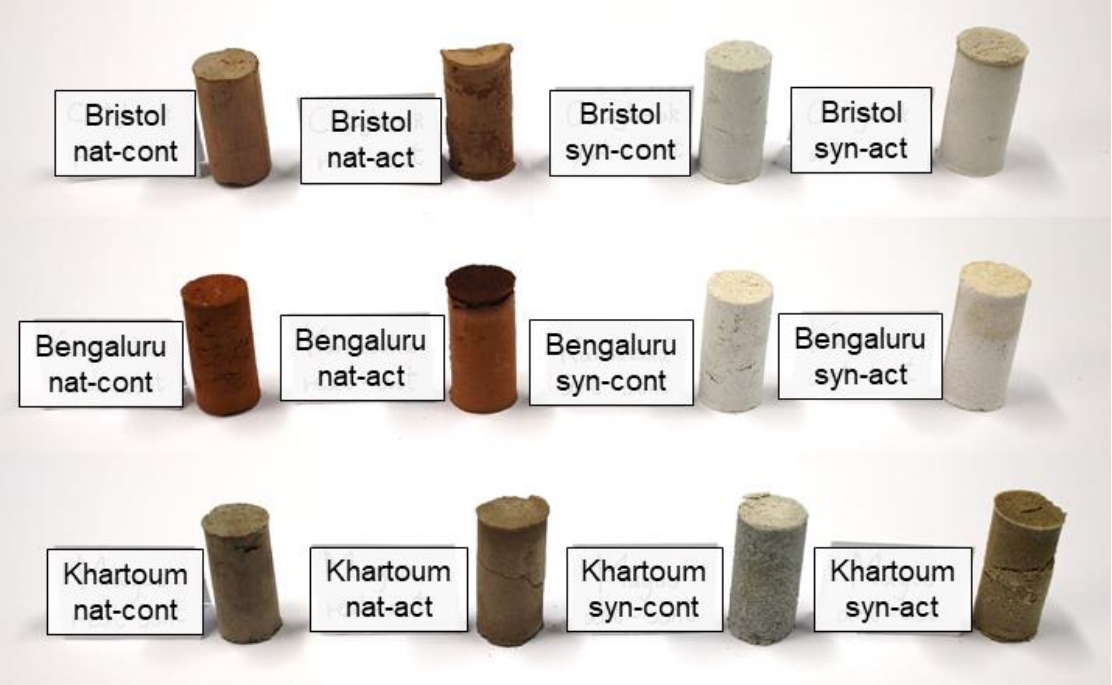

Figure 3: Photos of cured control and activated samples.

3.2 XRD

3.2.1 Precursors

The indexing of the Bristol and Khartoum natural soils was based on the quantitative analysis undertaken on these soils in previous studies [33, 34] (Figure 4a). XRD patterns were also measured for the <2 μm fraction of the soils, separated using a sedimentation technique [41], as this made some phases' peaks easier to resolve (Figure 4b). Regarding iron oxide/hydroxide compounds, hematite was identified as a probable phase in both Bristol-nat and Bengaluru-nat. The main hematite peak at 33.3 °2θ was weak, as expected given that it is typically present as very fine, disordered particles in soils However, given that both these soils demonstrated a noticeable response to an applied magnetic field [42], and that their colours were suggestive of hematite presence, from the collective evidence it was considered highly likely that hematite was present. The Khartoum-nat soil demonstrated a weak response to an applied magnetic field. Given its brown/grey colour, it may contain a small amount of fine goethite which was not detectable in XRD due to small size and low crystallinity [42, 43].

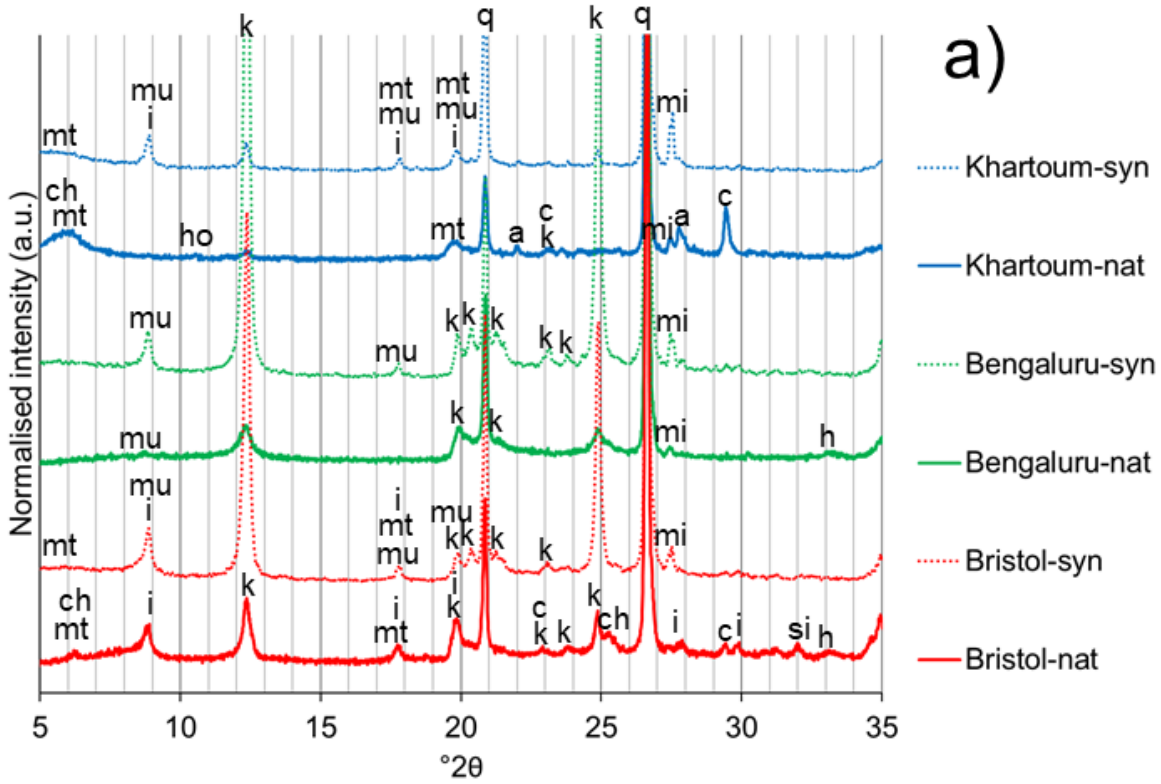

Clay minerals: **k** = kaolinite; **mt** = montmorillonite; **i** = illite.
Associated minerals: **a** = albite, **c** = calcite, **ch** = chlorite, **h** = hematite, **ho** = hornblende, **mi** = microcline, **mu** = muscovite, **q** = quartz, **si** = siderite.

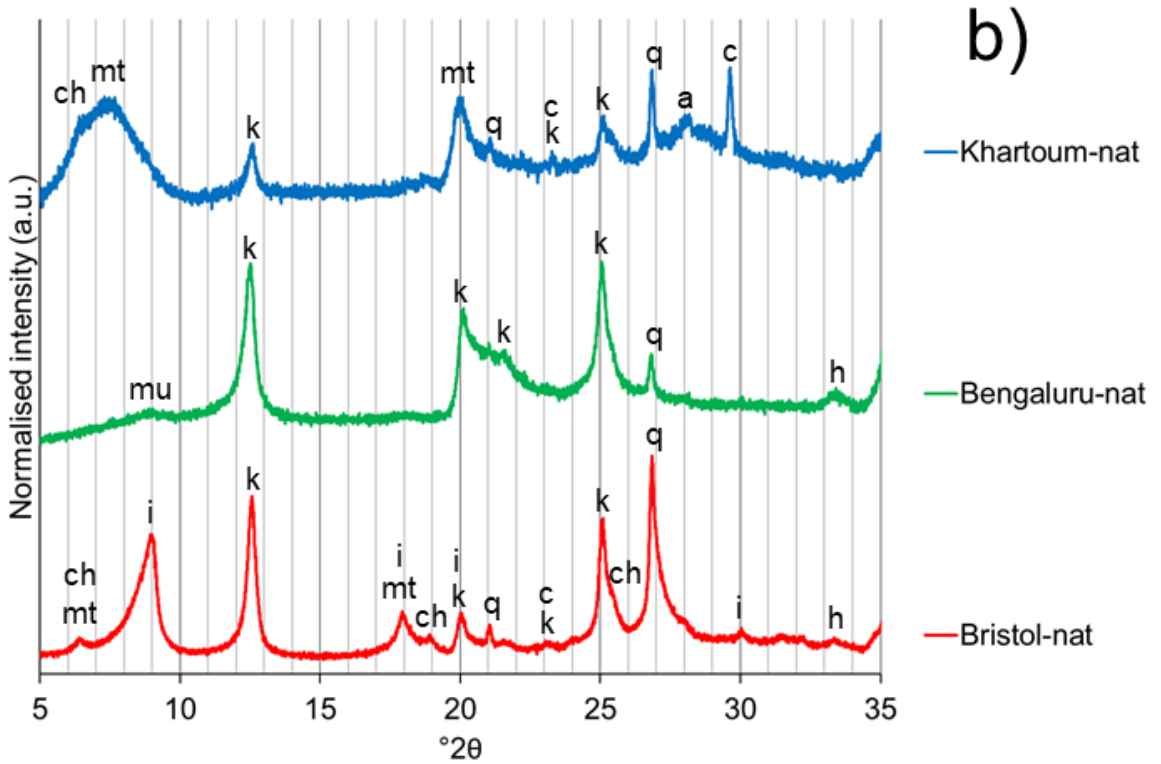

Figure 4: Indexed XRD patterns of the natural and synthetic soils: a) full size fraction, b) < 2 μm size fraction.

In the Bristol natural soil, the clay mineral phases present (listed in order of most to least abundant) were kaolinite (Powder Diffraction File (PDF)# 01-079-1570), illite (PDF# 00-026-0911) and montmorillonite (PDF# 00-013-0135), with quartz (PDF# 00-046-1045), hematite (PDF# 00-033-0664), a chlorite (PDF# 01-085-2163), calcite (PDF# 00-005-0586) and siderite (PDF# 00-029-0696) also present. In the synthetic soil, the same clay phases were present, with quartz, muscovite (PDF# 01-084-1304) and microcline (PDF# 00-019-0932) present as impurities.

In the Bengaluru natural soil, kaolinite was the only clay mineral present, with quartz, hematite, microcline and a mica phase also present. The mica phase was assigned as muscovite, given that the underlying geology of the area was granitic. In the synthetic soil, kaolinite was the sole clay mineral phase, with quartz, microcline and muscovite present as impurities. The broader profile of the kaolinite reflections is likely due to weathering in lateritic soils [43, 44].

In the Khartoum natural soil, the clay mineral phases present (listed in order of most to least abundant) were montmorillonite, kaolinite and illite, with quartz, microcline, a chlorite (PDF# 01-074-1137), albite (PDF# 00-009-0466), calcite and hornblende (PDF# 01-071-1060) also present. Given the high iron content of this soil (Table 1), at least one iron oxide or hydroxide phase was also expected to be present. Although reflections for these could not identified in the measured pattern, this might be expected as its reflections are generally weak due to its small size of typically 10 - 100 nm [42], and also given the number of other phases' reflections in the pattern. In the synthetic soil, the same clay phases were present, with quartz, microcline and muscovite present as impurities. The d-values of the 001 montmorillonite peak were 14.7 and 14.5 Å for the natural and synthetic soils respectively. This suggests their interlayer cations were Ca^{2+} and/or Mg^{2+} [45]. The montmorillonite clay used in the Khartoum synthetic soils had broad, diffuse diffraction peaks, and so is not obviously visible in the patterns for these soils.

In the following figures, only the main reflections for the clay minerals and reflections for product phases are indexed. This is done for purposes of clarity, given the number of associated mineral phases, and their general lack of observed reactivity.

3.2.2 Bristol Soils

In the natural soil, activation resulted in emergence of new reflections attributed to hydrosodalite $Na_6[AlSiO_4]_6 \cdot 4H_2O$ (PDF# 00-042-0216) (Figure 5). For the clay minerals: there was a reduction in intensity of the kaolinite reflections; the illite reflections did not seem not to decrease, and the montmorillonite reflection was too weak to discern any change,

especially given its overlap with a chamosite reflection. No notable changes were observed for any of the associated minerals' reflections.

In the synthetic soil, activation also resulted in emergence of new reflections attributed to basic hydrosodalite $Na_8[AlSiO_4]_6(OH)_2 \cdot 4H_2O$ (PDF# 00-041-0009). For the clay minerals there was: a reduction in intensity of the kaolinite reflections; the illite/muscovite reflections seemed to reduce in intensity, and again the montmorillonite reflection was too weak to discern any change. With regard to the minor phases, microcline's strongest reflections seemed also to reduce in intensity relative to the strongest quartz reflection.

Although particle orientation may have some influence, the intensity is less and the breadth is greater of the kaolinite 001 reflection (12.4 °2θ) in the natural soil compared to the synthetic soil. This could be due to particle-size broadening, suggesting that the kaolinite clay mineral phase may have a much smaller average crystallite size in the natural soil, although it is possible strain broadening could contribute too [40].

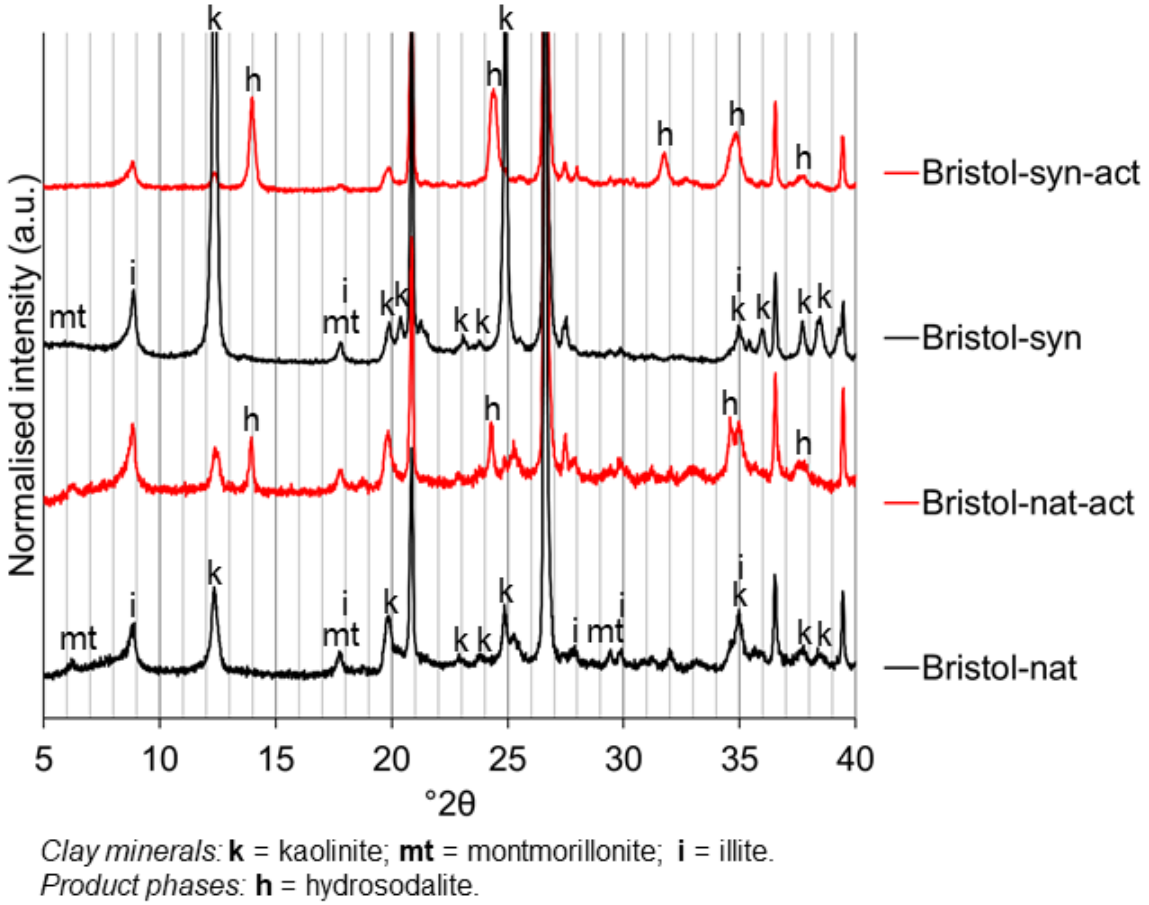

Figure 5: XRD patterns of the precursors and activated samples of the natural and synthetic Bristol soils

3.2.3 Bengaluru Soils

In the natural soil, activation resulted in emergence of new reflections attributed to the hydrosodalite $Na_6[AlSiO_4]_6 \cdot 4H_2O$ (PDF# 00-042-0216) (Figure 6). The reflections of kaolinite, the sole clay mineral present, decreased in intensity after activation. With regard to other phases, the weak reflection of hematite at 33.2 °2θ is still present after activation, whilst the main reflection of muscovite at 8.9 °2θ is too weak to be conclusive.

In the synthetic soil, activation resulted in emergence of new reflections also attributed to the hydrosodalite $Na_6[AlSiO_4]_6 \cdot 4H_2O$ (PDF# 00-042-0216). The reflections of kaolinite decreased in intensity after activation. The muscovite 002 and 004 reflections at 8.9 and 17.8 °2θ seemed to decrease relative to the most intense quartz reflection.

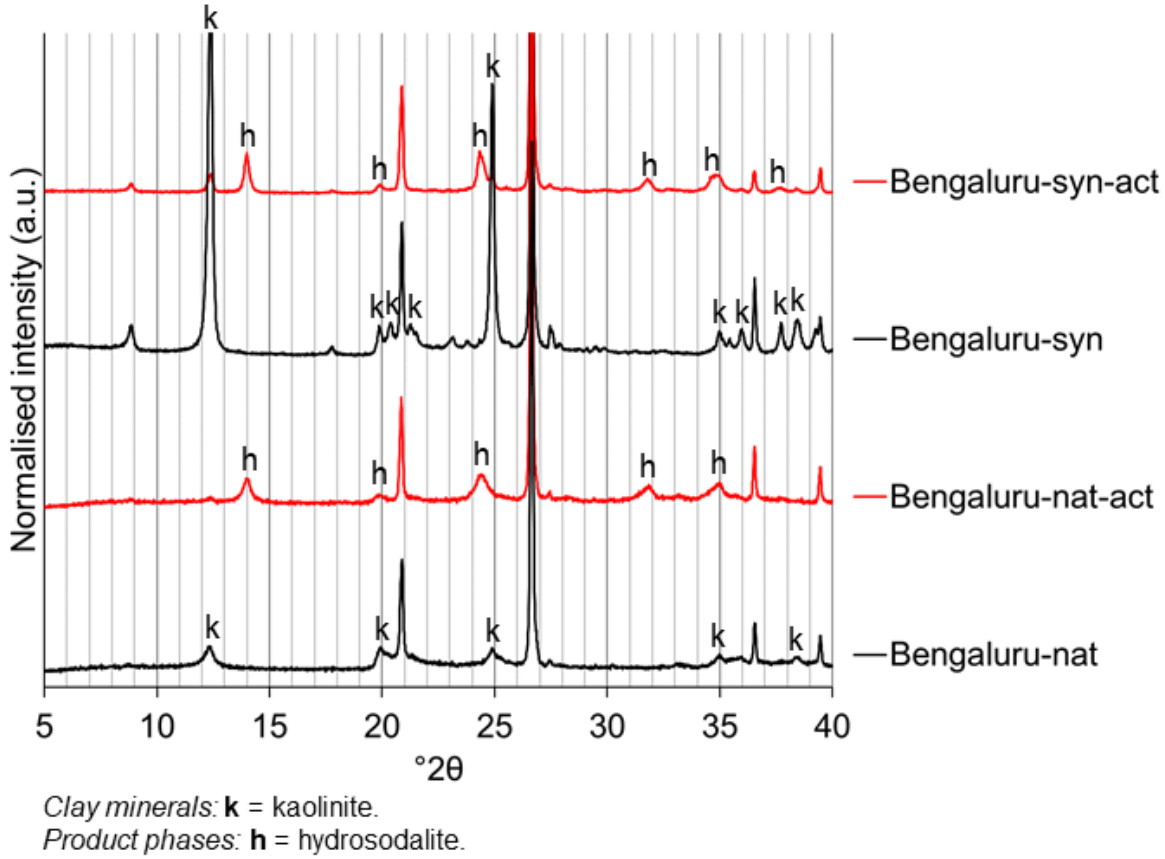

Figure 6: XRD patterns of the precursors and activated samples of the natural and synthetic Bengaluru soils.

3.2.4 Khartoum Soils

In the natural soil, activation resulted in no discernible formation of crystalline product phases (Figure 7). For the clay minerals, there was a shift of the montmorillonite 001 reflection from 5.9 to 7.3 °2θ, and hence a decrease in d-value from 15.0 to 12.1 Å. This shift has previously been attributed partly to interlayer cation exchange of Na^+ for Ca^{2+}/Mg^{2+}, and partly to the activation process itself [25]. This interpretation was consistent with a noticeable

decrease in plastic limit when NaOH concentration was increased (Figure 2), which is typical of Ca^{2+} montmorillonite [46]. The 001 reflection became broader after activation, making it unclear whether there was any change in overall intensity. The kaolinite 001 reflection (12.4 °2θ) did not undergo any noticeable change, and the illite reflections were too weak to say anything conclusive. No notable changes were observed for any of the associated minerals' reflections.

In the synthetic soil, activation also resulted in no visible formation of crystalline product phases. For the clay minerals, there were also the effects of cation exchange and activation process on montmorillonite, which underwent a shift of the 001 reflection from 5.6 to 7.2 °2θ, and hence a decrease in d-value from 15.8 to 12.3 Å. The montmorillonite 001 reflection also seemed to undergo a decrease in intensity. The kaolinite and illite/muscovite reflections seemed to decrease in intensity in comparison to the main quartz reflection. With regard to minor phases, the microcline reflection at 27.5 °2θ seemed to undergo a decrease in intensity.

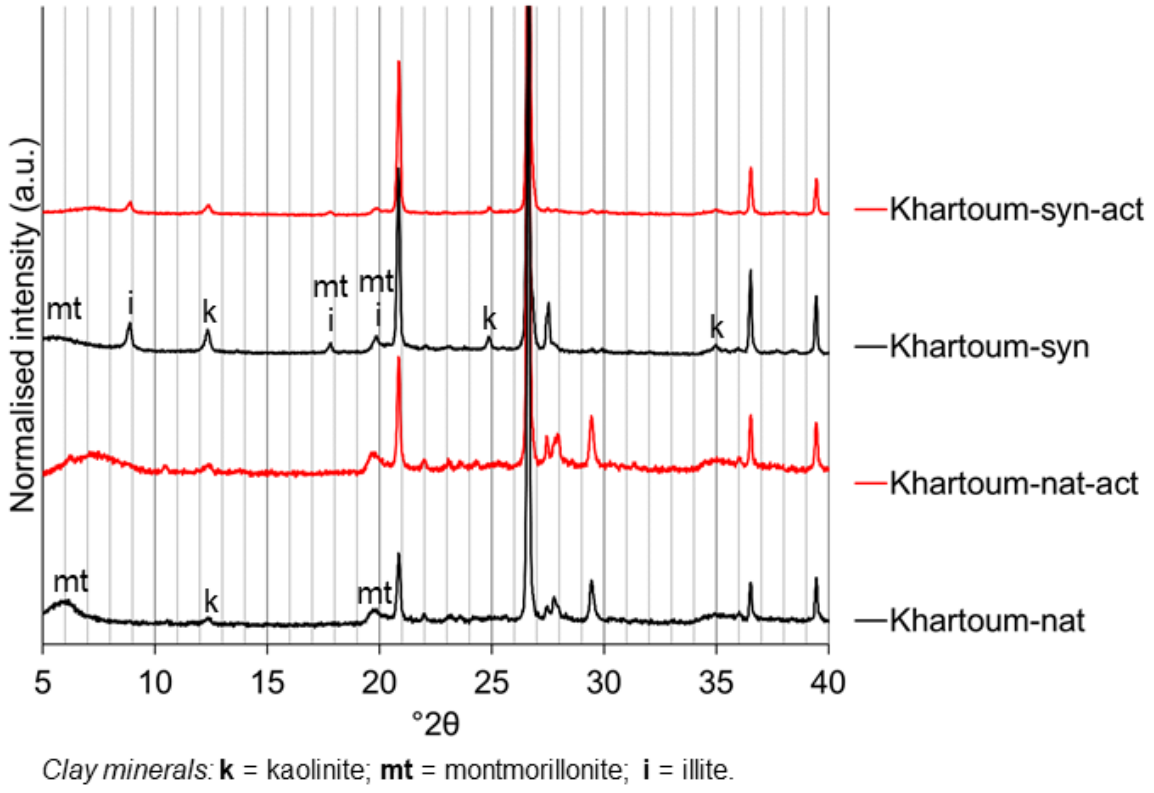

Figure 7: XRD patterns of the precursors and activated samples of the natural and synthetic Khartoum soils.

3.3 SEM

3.3.1 Bristol Soils

The micron-scale clay platelets were clearly visible in the images of both the natural and synthetic control samples (Figure 8). In the activated natural soil, there were still a large number of clay particles visible, and also some new particles of typical size ~0.5 µm were observed. In the activated synthetic soil, only a small number of clay particles were still present. The microstructure was dominated by new particles of typical size ~0.2 µm – these were attributed to the hydrosodalite phase identified in the XRD pattern, as they had a typical morphology for hydrosodalites [47].

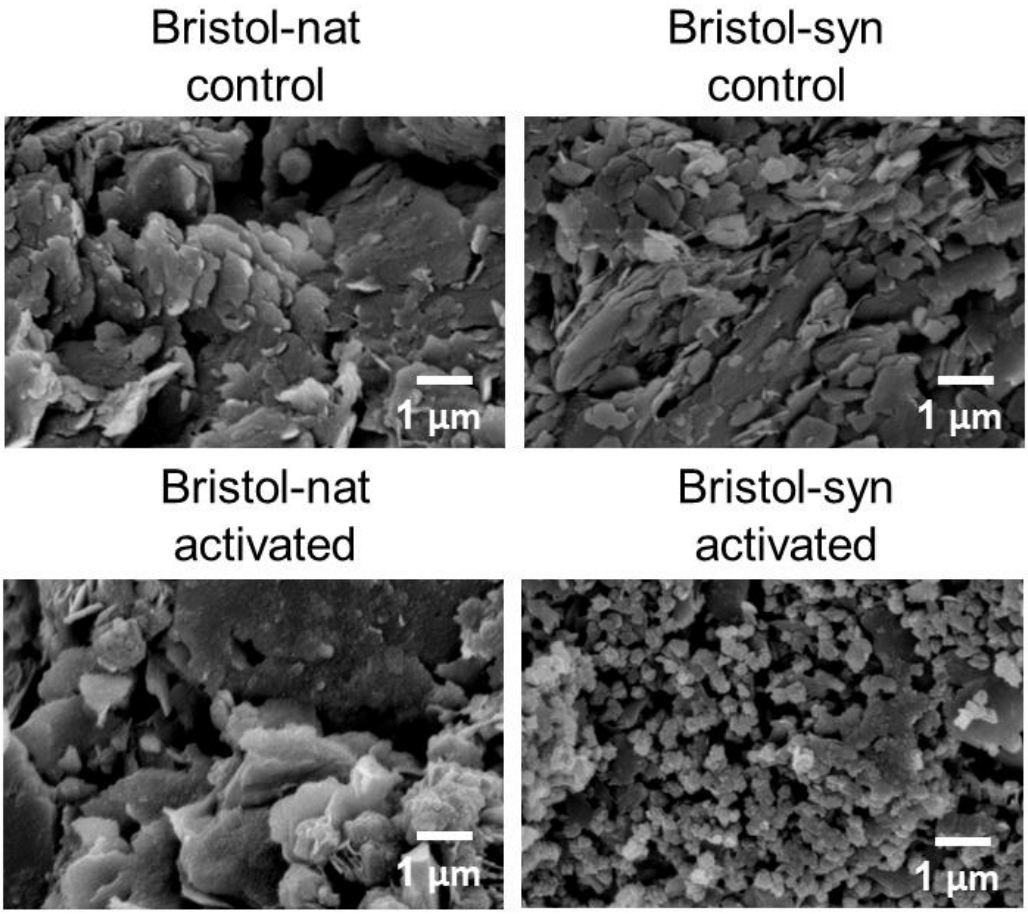

Figure 8: SEM images of control and activated samples of the natural and synthetic Bristol soils.

3.3.2 Bengaluru Soils

The micron-scale clay platelets are clearly visible in the image of the synthetic control sample (Figure 9). In the image of the natural control sample, the scale of the particles was much finer, typically <0.1 µm. This observation agrees with the BET SSA values given in Section 2.1, which were significantly higher for the natural control soil.

In the activated natural soil, the microstructural features were of a similar scale to the control sample. This made differences in phase morphology inconclusive, although the size distribution of fine particles increased from <0.1 µm to 0.1 - 0.2 µm. This difference in particle size distribution was attributed to the transformation of kaolinite into a hydrosodalite phase, as identified in the XRD pattern. In the activated synthetic soil, a small number of clay particles were still present. The microstructure was dominated by new particles of typical size ~0.3 µm, attributed to the hydrosodalite phase identified in the XRD pattern, as similarly observed in the Bristol-syn-act system.

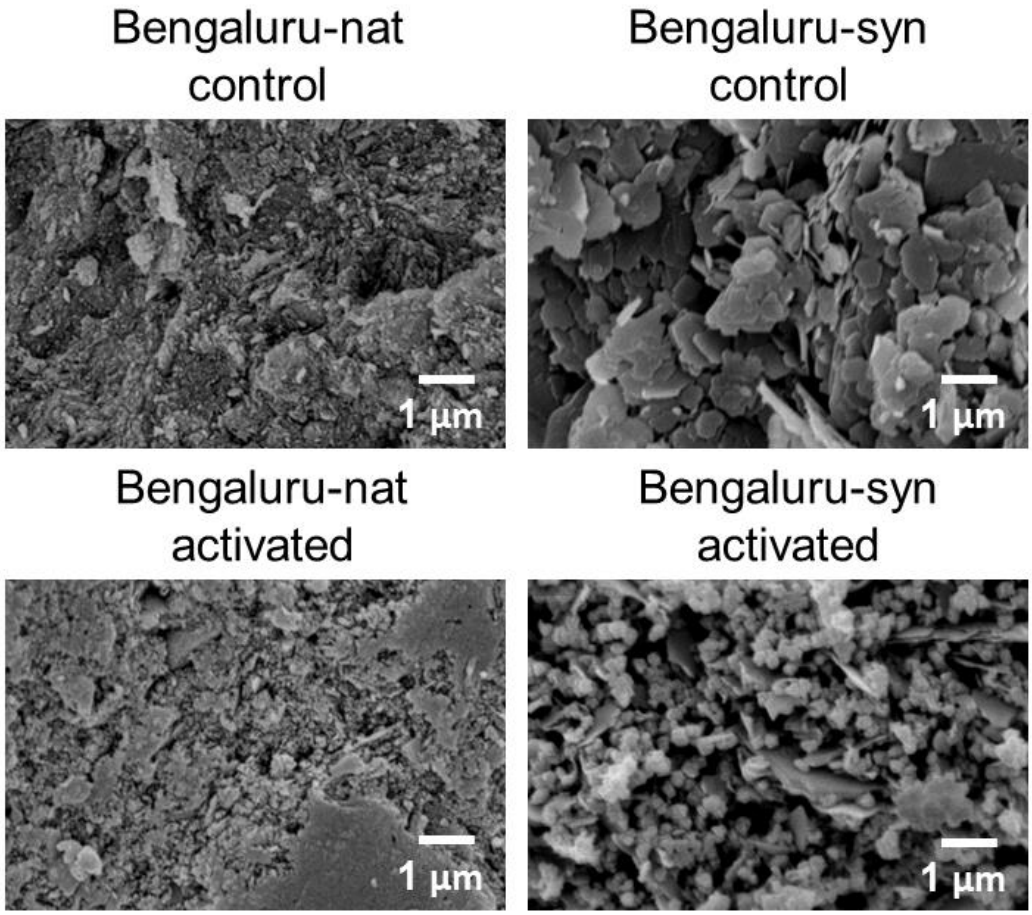

Figure 9: SEM images of control and activated samples of the natural and synthetic Bengaluru soils.

3.3.3 Khartoum Soils

The micron-scale clay platelets were clearly visible in the images of both the natural and synthetic control samples (Figure 10). In the image of the activated natural soil, the edges of the platy particles appeared with ragged edges, suggestive of the edge-dominated dissolution mechanism of these clays in alkaline solutions [48, 49]. No new microstructural features were observed. In the image of the activated synthetic soil, irregular particles of typical size ~0.5 µm were evenly distributed in the microstructure. This was similar to the microstructure previously observed for an activated mixture of 90% montmorillonite and 10% kaolinite clays [32]. These are unlikely to be individual zeolitic particles - they do not exhibit the expected angular morphology [47], and given that no zeolitic reflections were observed in the XRD patterns, they are too large to be x-ray amorphous zeolites [50]. This suggests these could either a poorly linked geopolymer phase or carbonate precipitates.

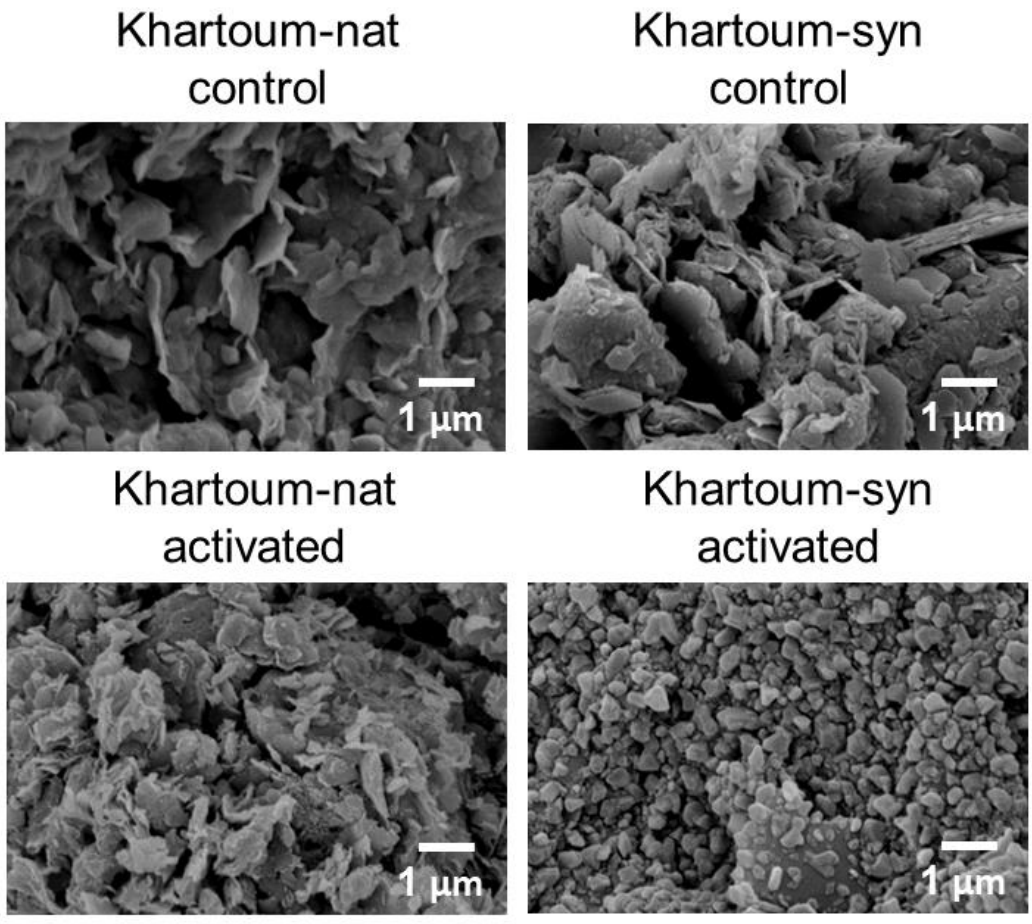

Figure 10: SEM images of control and activated samples of the natural and synthetic Khartoum soils.

3.4 FTIR

The range 2000 - 600 cm^{-1} is displayed - this is the range of most interest as it contains the stretching bands of the aluminosilicate and alkali aluminosilicate phases.

3.4.1 Bristol Soils

There were no significant differences between the FTIR spectra of the natural and synthetic soils' control samples (Figure 11). The same bands were present, albeit with small differences in relative intensity. The position of the dominant Si-O-Si stretching vibration was slightly higher for the synthetic soil (1006 cm^{-1}) than the natural soil (1000 cm^{-1}).

The changes in the dominant aluminosilicate band were similar for both natural and synthetic soils, with a broadening and shift to lower wavenumbers (984 and 979 cm^{-1} respectively). Broad carbonate bands, likely composed of several superimposed bands emerged for both soils centred at ~1450 cm^{-1}, along with another individual band at 850 - 865 cm^{-1}. These were more intense for the natural soil.

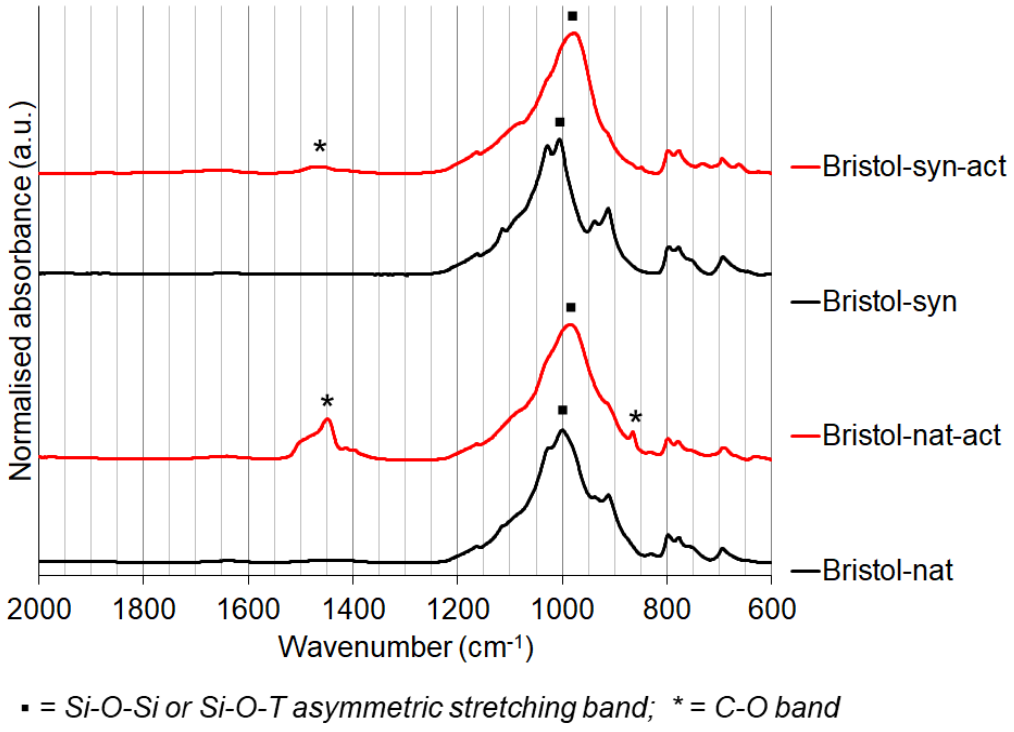

Figure 11: FTIR spectra of precursor and activated samples of the natural and synthetic Bristol soils.

3.4.2 Bengaluru Soils

There were no significant differences between the FTIR spectra of the natural and synthetic soils' control samples (Figure 12). The same bands were present, albeit with small differences in relative intensity. The position of the dominant Si-O-Si stretching vibration was slightly higher for the synthetic soil (1006 cm^{-1}) than the natural soil (1004 cm^{-1}).

The changes in the dominant aluminosilicate band were similar for both natural and synthetic soils, with a broadening and shift to lower wavenumbers (976 and 979 cm^{-1} respectively).

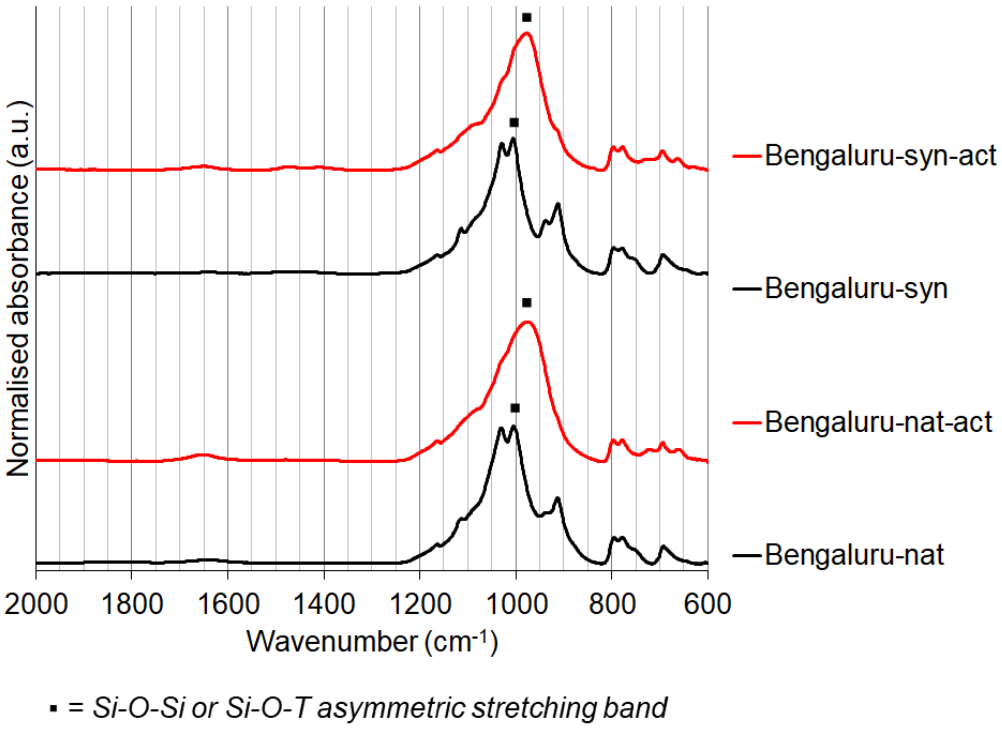

Figure 12: FTIR spectra of control and activated samples of the natural and synthetic Bengaluru soils.

3.4.3 Khartoum Soils

Due to larger differences in relative intensity between the different aluminosilicate bands in the control samples' spectra, the position of the dominant Si-O-Si stretching vibration was significantly lower in the natural soil (1003 cm^{-1}) than in the synthetic soil (1032 cm^{-1}) (Figure 13). Carbonate bands at ~1450 cm^{-1} and 873 cm^{-1} were only present in the natural soil's control spectrum, attributed to calcite.

The changes in the dominant aluminosilicate band were similar for both natural and synthetic soils, undergoing broadening but also a very small shift in wavenumbers compared to the other soils (1004 and 1031 cm^{-1} respectively). The calcite carbonate bands remained present for the natural soil, and weaker carbonate bands emerged in the same locations for the synthetic soil. A broad carbonate band, also centred at ~1450 cm^{-1}, emerged for the synthetic artificial soil after activation, along with another individual band at ~865 cm^{-1}.

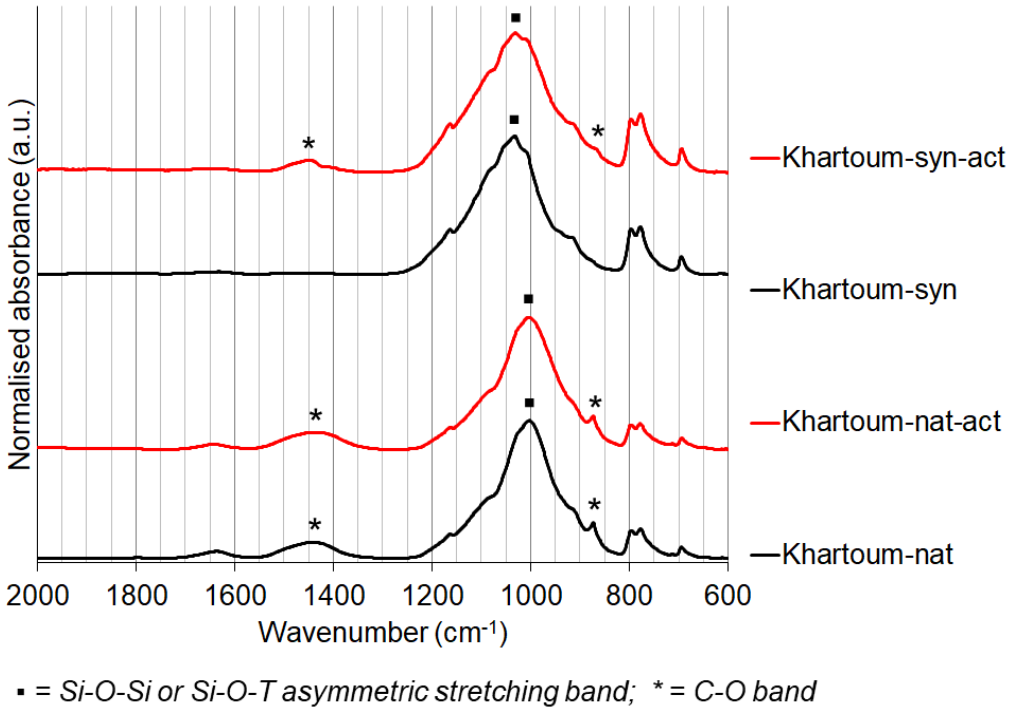

Figure 13: FTIR spectra of control and activated samples of the natural and synthetic Khartoum soils.

3.5 TGA

Most of the minerals known to be present in the soils undergo some form of mass loss event in the temperature range tested, as follows [51, 52]. Clay minerals can be distinguished by their dehydroxylation temperatures, which typically lie within the range of 450 – 750 °C. For the silicates and other aluminosilicates, dehydroxylation typically occurs in a higher range. The exceptions are quartz and microcline, which do not contain hydroxyl groups. For the carbonates, decomposition typically occurs from 700 – 960 °C. For the iron oxides and

hydroxides, some only undergo decomposition rather than structural changes. These specificities make TG and dTG curves particularly helpful for confirming the identity of minerals in soil.

As shown in the FTIR results (Section 3.4), it is likely that due to efflorescence, small amounts of sodium carbonate phases were present in the activated soils which were not detected in the XRD patterns. The phases most likely to be present are natrite (Na_2CO_3), thermonatrite ($Na_2CO_3 \cdot H_2O$) and trona ($Na_3H(CO_3)_2 \cdot 2H_2O$). For the latter two compounds, dehydration and/or partial carbon loss can occur < 300 °C, to form natrite [51, 53]. Full decomposition of natrite occurs above 840 °C [54].

Due to the complex phase composition of these soils and the possibilities of overlapping loss peaks, it was not always possible to provide a complete indexing of the dTG curves. dTG peaks will be described either by their peak centre if well-resolved, or approximate temperature range if not.

3.5.1 Bristol Soils

In the dTG curves of the natural / synthetic precursor soils (Figure 14), the mass loss events were attributed to the following phases: 102 / 92 °C to the loss of surface adsorbed water from clay minerals; the largest magnitude peaks at 490 / 507 °C to the dehydroxylation of kaolinite and montmorillonite; 645 °C to the dehydroxylation of illite in the natural soil [51, 55]. In the natural soil, the small peak at 309 °C was assigned to the dehydration of hydrate phases associated with hematite [56], and the peak at 644 °C to decomposition of calcite [57]. In the synthetic soil, the shoulder at 656 °C could possibly have been due to a trace amount of calcite in the sand addition. The major dTG loss peaks expected from the other associated minerals were either overlapping with the larger clay minerals' peaks, or not of large enough magnitude to be assigned with confidence. The overall mass loss was slightly greater for the natural precursor soil (-7.0 %) than for the artificial one (-4.9 %).

In the activated samples of both the natural and artificial soils, there was a large decrease in the magnitude of the kaolinite dTG peak, in agreement with the consumption of kaolinite shown in the XRD patterns (Figure 5). In the activated natural soil, broad peaks emerged at 212, 315 and 394 °C, which overlapped in the 100 - 400 °C region. The magnitude of the 89 °C surface adsorbed moisture peak increased greatly. In the activated synthetic soil, there was also a large decrease in magnitude of the kaolinite dTG peak. New, broad peaks emerged at 160 °C and elsewhere within the 100 - 400 °C region. There was also a large increase of the surface adsorbed moisture peak at 102 °C.

The new peaks in the 100 - 400 °C region for both activated samples were attributed to zeolitic water loss from the respective hydrosodalites identified in the XRD patterns. Peaks in this region are indicative of hydrosodalites, with the loss temperature and number of the dTG peaks corresponding to H_2O and/or OH loss from the β-cages [58]. The clear difference in the profile of the dTG curves in this region would therefore be expected from the formation of a basic and non-basic hydrosodalite. The increase in surface-adsorbed moisture loss at ~100 °C was also attributed to the presence of hydrosodalites.

In both activated soils, the dTG intensity increased in the 700 - 1000 °C region. This could partly be attributed to the decomposition of natrite (Na_2CO_3), but only in the range of >840 °C. In the TG curves, overall mass loss increased after activation for both soils but to a greater extent for the natural soil (2.1 %) than for the synthetic soil (0.7 %).

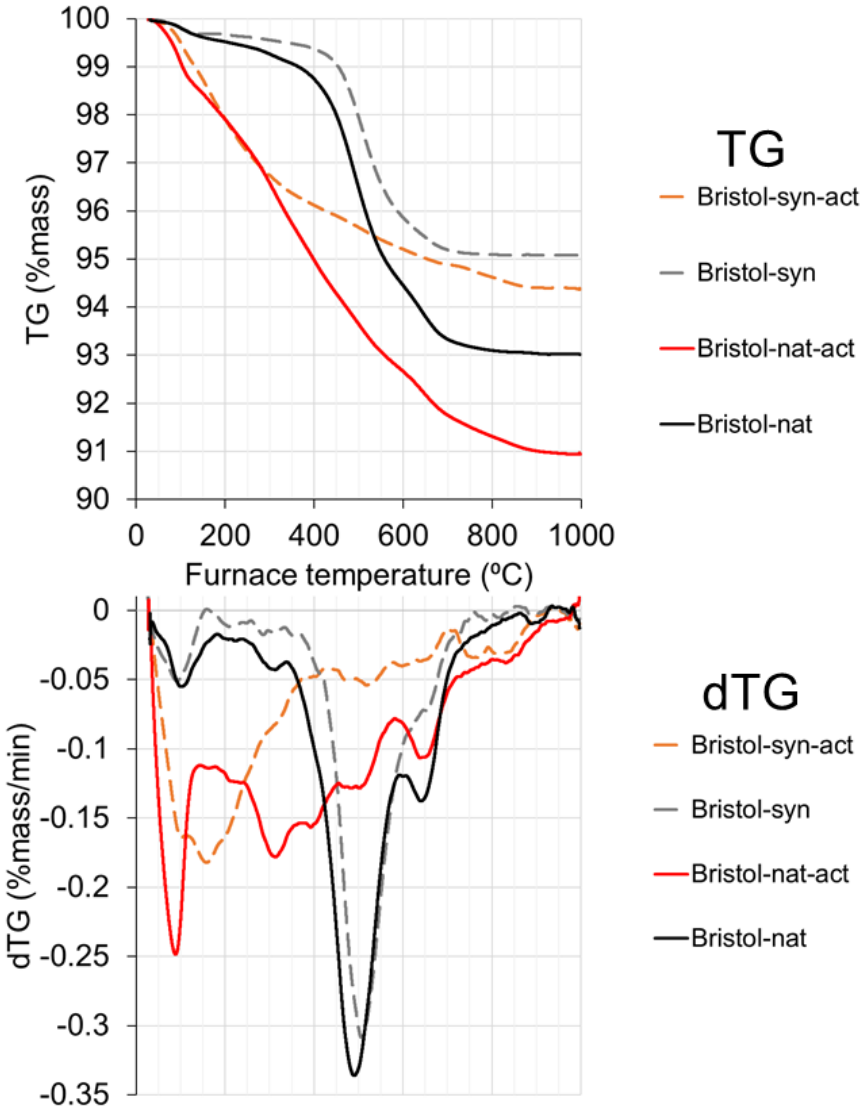

Figure 14: TGA and dTG spectra of control and activated samples of the natural and synthetic Bristol soils.

3.5.2 Bengaluru Soils

In the dTG curves of the natural / synthetic precursor soils (Figure 15), the mass loss events were attributed to the following phases: 87 / 105 °C to the loss of surface adsorbed water from clay minerals; the largest magnitude peaks at 458 / 508 °C to the dehydroxylation of kaolinite [51, 55]. In the natural soil, the small peak at 289 °C was assigned to the dehydration of hydrate phases associated with hematite [56]. In the synthetic soil, the shoulder at 618 °C could possibly have been due to a trace amount of calcite in the sand addition. The overall mass loss was slightly greater for the natural precursor soil (-6.8 %) than for the artificial one (-5.2 %).

In the activated samples of both the natural and artificial soils, there was a large decrease in the magnitude of the kaolinite dTG peak, in agreement with the consumption of kaolinite shown in the XRD patterns (Figure 6). In the activated natural soil, broad peaks emerged at 198 and 287 °C. The magnitude of the 111 °C surface adsorbed moisture peak increased greatly. The hematite peak was still present after activation. In the activated synthetic soil, a new peak emerged at 197 °C, with another possibly in the overlapping region from 100 – 200 °C. There was also a large increase of the surface adsorbed moisture peak.

The new peaks in the 100 - 200 °C range were attributed to the non-basic hydrosodalite identified in the XRD patterns (Figure 6). The broad similarity in number and locations of loss peaks in this temperature range between the activated soils is in agreement with the observation that the same type of hydrosodalite was formed in both samples. The increase in surface-adsorbed moisture loss was also attributed to the presence of hydrosodalites.

In the activated synthetic soil, minor, broad peaks also emerged at 658 and 759 °C. In contrast, there was negligible change for the activated natural soil in this temperature range. In the TG curves, overall mass loss did not change after activation for the real soil, but decreased a slight amount for the synthetic soil.

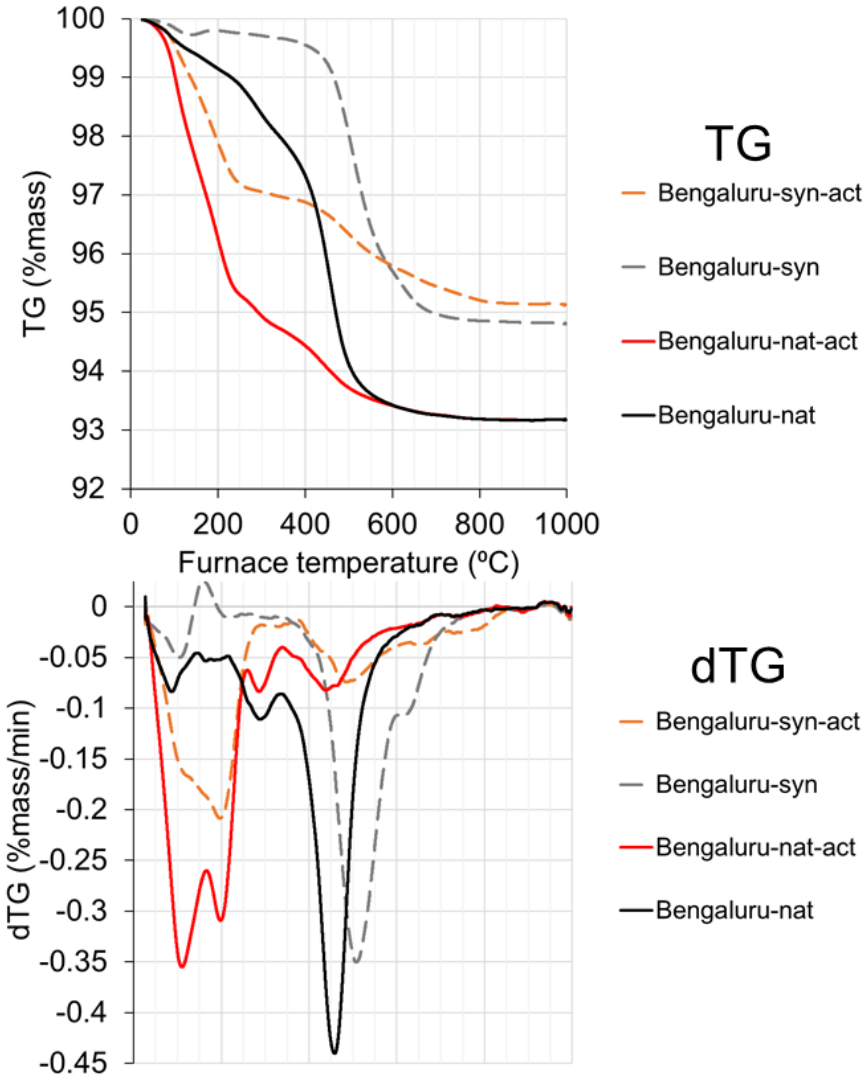

Figure 15: TGA and dTG spectra of control and activated samples of the natural and synthetic Bengaluru soils.

3.5.3 Khartoum Soils

In the dTG curves of the natural / synthetic precursor soils (Figure 14), the mass loss events were attributed to the following phases: 88 / 78 °C to the loss of surface adsorbed water from clay minerals; the largest magnitude peaks at 471 / 496 °C to the dehydroxylation of montmorillonite [51, 55]. Both these dehydroxylation temperatures are in the lower end of the range for montmorillonites, suggesting that both had a trans-vacant octahedral sheet structure [59, 60]. In the natural soil only, mass loss peak attributions were: 285 °C to the dehydration of hydrate phases associated with hematite [56]; 696 °C to the decomposition of calcite [57]. The montmorillonite dehydroxylation peak at 471 °C exhibited a shoulder on the lower temperature side - after activation, a peak was visible at 421 °C. This peak could be the dehydroxylation of goethite (FeOOH) [51], a common iron compound in soils [42]. However, it was not possible to confirm this attribution through XRD due to the fine size distribution and low crystallinity of iron compounds in soil, as previously described in Section

3.2.1. In the synthetic soil only, the peak at 656 °C could have been due to decomposition of a trace amount of calcite in the sand addition. The overall mass loss was greater for the natural precursor soil (-10.0 %) than for the artificial one (-2.5 %).

In the activated natural soil, there was a decrease in magnitude of the montmorillonite dehydroxylation peak at 471 °C. In the activated synthetic soil, there seemed to be a decrease in magnitude of the equivalent peak at 496 °C. In the activated natural soil, there was almost no change in the surface adsorbed moisture peak, whereas in the synthetic activated soil there was a large increase in magnitude of the equivalent peak.

In the activated natural soil, a new minor peak emerged at 774 °C. The calcite peak, and possible hematite and goethite peaks, were still present after activation. In the synthetic activated soil there was negligible change in the 750 - 1000 °C range, but there was a broad increase in magnitude from 170 - 400 °C. From a previous study on a montmorillonite system [25], this phenomenon is associated with the presence of a geopolymer. In the TG curves, overall mass loss decreased (-0.7%) for the natural soil, but increased for the synthetic soil (1.5 %).

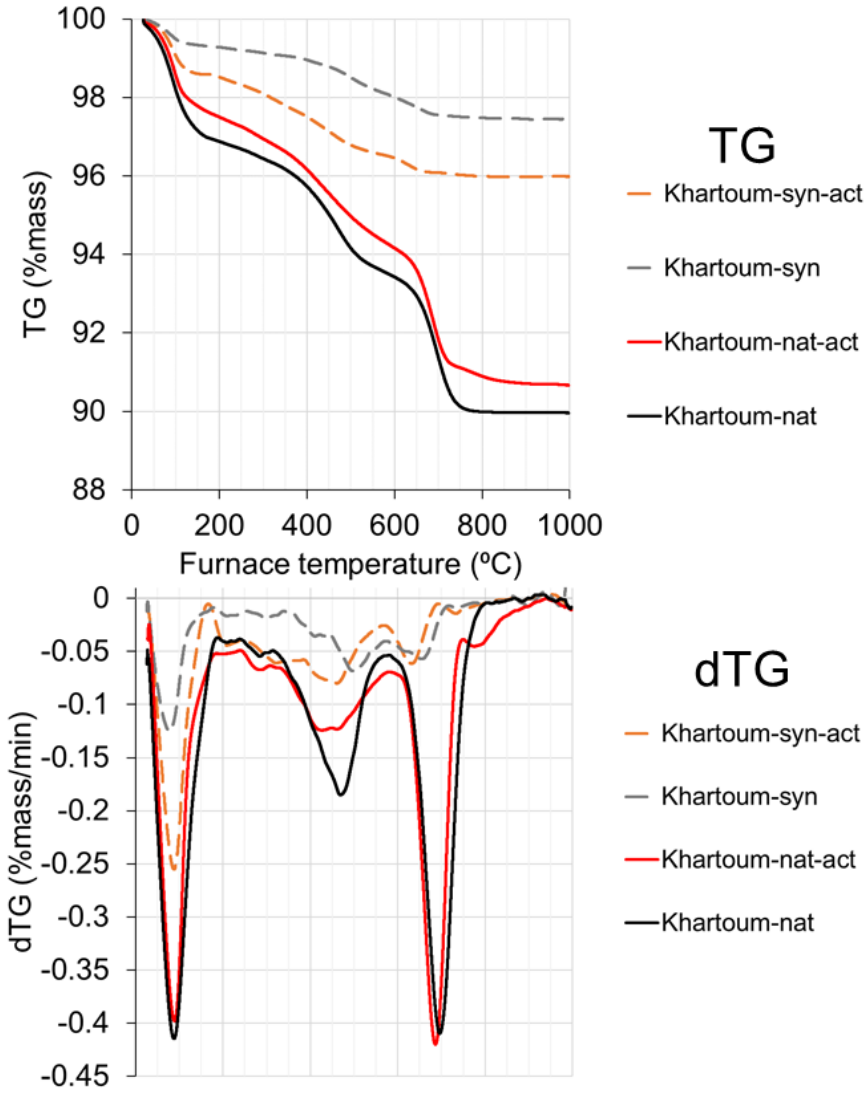

Figure 16: TGA and dTG spectra of control and activated samples of the natural and synthetic Khartoum soils.

4 Discussion

4.1 Phase formation for natural and synthetic soils

There were both similarities and differences between the phases formed in the natural and synthetic versions of each soil, as summarised in Table 5.

Table 5: Summary table showing phases formed from activation of the natural and synthetic soils.

Soil	Natural	Synthetic
Bristol	hydrosodalite	basic hydrosodalite
Bengaluru	hydrosodalite	hydrosodalite
Khartoum	none	geopolymer

As expected for a kaolinite dominated soil [31], for the Bristol soils, hydrosodalite was formed as the reaction product in both the natural and synthetic soils. However, different hydrosodalities were formed in each of the soils: a non-basic hydrosodalite $Na_6[AlSiO_4]_6 \cdot 4H_2O$ in the natural soil, and a basic hydrosodalite $Na_8[AlSiO_4]_6(OH)_2 \cdot 4H_2O$ in the synthetic soil. The existence of different product phases is supported by differences in the TGA and FTIR signals, as already described in Sections 3.5.1 and 3.4.1. The difference in the scale of the clay phases, predominantly kaolinite, was negligible between the two precursor soils, as already shown from the BET specific surface area and SEM results in Sections 2.1 and 3.3.1. Previous studies on the synthesis of zeolites from kaolinite have shown that phase formation is sensitive to temperature, time, alkaline solution concentration and Si:Al ratio [61, 62]. It is therefore likely that this difference is either due to slight differences in the mineralogy of the kaolinite, or very minor variations in the processing and curing conditions.

For the Bengaluru soils, exactly the same hydrosodalite phase was formed in both the natural and synthetic soils, the non-basic hydrosodalite $Na_6[AlSiO_4]_6 \cdot 4H_2O$. The hydrosodalite particles formed were much finer in the activated natural soil, as already described in the SEM results in Section 3.3.2. In the precursor, the kaolinite particles were much smaller, and specific surface area much higher as already described in Sections 3.3.2 and 2.1. It is likely that the finer kaolinite particles offered a higher spatial density of nucleation sites, thus resulting in the formation of more, finer hydrosodalite particles.

For the Khartoum soils, no crystalline product phases were formed in either the natural or synthetic soils. A change of microstructure was observed in the SEM images which could have been a geopolymer (Section 3.3.3) as well as changes in the dTG spectrum indicative of geopolymer formation (Section 3.5.3), but the evidence was not conclusive given there was no large observed negative shift of the Si-O-T FTIR band after activation (Section

3.4.3). It is therefore likely that a small amount of poorly linked geopolymer N-A-S-H or (N,C)-A-S-H phase formed in the synthetic soil, but not for the natural soil. However, the results included in the Appendix show some evidence for geopolymer formation in both natural and synthetic soils when using 10 M NaOH. This suggests that in the lower concentration activation of the natural soil, geopolymer formation was retarded, but not prevented, relative to the synthetic soil.

In summary, in spite of the differences in particle size and the absence of minor non-clay minerals in the synthetic soils, the phase formation behaviour was generally similar between the natural and synthetic soils, albeit with non-clay components having a retarding effect in Khartoum-syn.

4.2 Evaluation of clay minerals in activation

In addition to characterising overall phase formation, the purpose of this study was to determine the relative influence of clay minerals and associated minerals in alkaline activation behaviour of soils.

The Bristol natural soil had a slightly larger specific surface area than the synthetic soil (17.6 to 14.0 m^2g^{-1}), but the difference in particle size distribution as seen from the SEM images was negligible (Figure 8). The Bengaluru natural soil had a significantly larger specific surface area and finer particle size than the synthetic soil (33.7 to 6.7 m^2g^{-1}), also seen in the SEM images (Figure 9). The kaolinite dTG mass loss peak was 50 °C lower for the natural soil than the synthetic soil, which is consistent with smaller particle size [63]. Accumulation of iron in kaolinite during pedogenic processes can make them more reactive by increasing disorder [23]. The decrease in intensity of the kaolinite 001 peak after activation was similar for the natural and synthetic soils, suggesting that the clays had similar reactivity and hence that the kaolinite in the natural soil had low iron accumulation and was still relatively ordered. The Khartoum natural soil had a similar surface area to the synthetic soil (36.9 to 42.0 m^2g^{-1}), and seemed similar in terms of size from the SEM images (Figure 10). Furthermore, the montmorillonite dehydroxylation temperatures suggested that the montmorillonite clay minerals in both soils had a trans-vacant octahedral sheet structure (Section 3.5.3). The sheet structure of montmorillonites is known to influence some behaviours such as dehydroxylation mechanism [59, 60], and also pozzolanic reactivity [37]. It was therefore desirable for getting an overall match between the clay minerals in the real and synthetic soils that both montmorillonite precursors had a trans-vacant structure. However, wavenumber of the Si-O-T FTIR band was ~30 cm^{-1} lower for the natural soil (Figure 13), and the dTG peak for montmorillonite dehydroxylation occurred at ~30 °C lower in the

natural soil (Figure 16). For the purpose of this exercise, the clay minerals in the synthetic soils were deemed to be suitable comparison points for those in the natural soils.

A previous study [32] investigated the alkali activation products of different clay mixtures under the same processing conditions used here. These are useful comparison systems, as they can be considered as simplified soil systems. The mixtures closest to the soils, and their phase formation behaviours, were: for Bengaluru, 100%Kao forming hydrosodalite; for Bristol, 50%Kao-50%ILL forming hydrosodalite and a minor amount of hydroxycancrinite, and for Khartoum, 90%Mont-10%Kao forming a geopolymer. These make an overall good agreement with the phases formed in the respective soils here. This is in agreement with the findings of the previous section, and supports the argument that phase formation behaviour is predominantly determined by the clay minerals.

4.3 Evaluation of associated minerals in activation

The associated minerals found in the natural soils included quartz, hematite, chlorite, siderite, muscovite, microcline, albite, calcite and hornblende. The synthetic soils were designed to match the natural soils in terms of clay content, but would not feature any of the minor phases found in the natural soils. In practice it was not possible to fully avoid these, since the precursor clays used for the synthetic soils contained small amounts of quartz, muscovite and microcline. Therefore, the behaviour of the associated minerals in all of the soil systems will be evaluated. The associated minerals can be categorised into two groups: firstly, silicate/aluminosilicate phases that might contribute directly to the alkali activation reaction through dissolution and donation of aluminium and/or silicon species (quartz, chlorite, muscovite, microcline, albite, hornblende); secondly, other phases which do not contain aluminium or silicon, but which might influence the system in other ways (hematite, siderite, calcite).

In the first group of aluminosilicate/silicate minerals, quartz is the most common associated mineral in soils, and typically the largest component of the silt and sand size fractions, albeit with a size distribution dependent on weathering conditions [29]. Given that quartz consistently has the most intense reflections in the XRD patterns (Figure 4), this is likely the case for all the precursor soils used here. It is therefore difficult to say whether any minor dissolution of quartz occurred, although quartz remained the largest peak after activation for all soils. However, given the curing conditions used [64], and the presence of more reactive minerals, it is unlikely that anything more than a minor amount of quartz dissolution occurred.

Feldspars are the second most common associated mineral in soils [29], and include the alkali feldspar (including microcline) and plagioclase (including albite) sub-groups.

Microcline's most intense XRD reflection seemed to undergo a decrease in intensity after activation in all the synthetic soils (Figure 5, Figure 6, Figure 7), but not in Bengaluru-nat, the only natural soil in which microcline was present (Figure 6). Albite was present in the precursor of Khartoum-nat, but did not undergo any noticeable decrease (Figure 7). In comparison with previous studies, Xu and van Deventer [65] found that aluminosilicates with a ring structure – including feldspars – had a lower extent of dissolution than minerals with framework or chain structures. The same researchers later activated uncalcined albite and microcline, and found that both formed a geopolymer when in a mixture with kaolinite [66]. In comparison, Feng et al. [67] found that albite in isolation had little ability to form a geopolymer phase when activated in its uncalcined or calcined state, albeit without additional silicate. No hard conclusions can be drawn on the exact extent of participation of feldspars in these specific systems, except that there seems to be variation between feldspars, and that they do not have a deleterious effect on overall phase formation behaviour.

Amongst micas, muscovite is a common minor component in soils [29]. Muscovite was present in all the synthetic soils (through its presence in the kaolinite precursor), and also in Bengaluru-nat. Discerning any changes in muscovite reflections in the XRD patterns of Bristol-syn and Khartoum-syn was not feasible, as they overlapped with the other 2:1 phyllosilicates montmorillonite and/or illite. In the Bengaluru soils, kaolinite was the sole clay mineral, and hence did not overlap (Figure 6). In Bengaluru-nat, the intensity of the muscovite reflection was too weak to discern any change with confidence, whereas in Bengaluru-syn, there seemed to be a clear decrease. It is within reason that this change could be partly explained by orientation effects.

Chlorites are unstable in soil environments, but can be found as an inherited mineral [29]. In Bristol-nat, both the main reflection at 6.2 and 25.2 °2θ were retained after activation (Figure 5). In Khartoum-nat, the reflection at 6.2 °2θ was also retained after activation. In Khartoum-nat, the only soil containing a hornblende, the main reflection at 10.5 °2θ was retained (Figure 7).

In the second group of non-aluminosilicate/silicate minerals, iron compounds are found to some extent in nearly all soils, with goethite (α-FeOOH), hematite (α-Fe_2O_3) and magnetite (Fe_3O_4) the most widespread [29]. Their size distribution is in the <2 μm clay fraction [42]. The presence of iron phases in lateritic soils is of additional interest because of their known surface hardening effect under conditions of wetting and drying cycles [21, 68]. Iron compounds were only found in the natural soils. As shown in Table 1, iron oxide composition differed by up to 10 wt.% between the natural and synthetic soils. Hematite was present in

Bristol-nat and Bengaluru-nat, with possibly a small amount of goethite present in Khartoum-nat as described in Section 3.2.1. Hematite's main reflection at 33.2 °2θ seemed to decrease in intensity after activation in both Bristol-nat and Karnatak-nat. Hematite has low solubility in alkaline solutions, but does increase with concentration [69]. Siderite was only present in Bristol-nat, and its main reflection at 32.0 °2θ decreased in intensity after activation. The iron phase (likely goethite) in Khartoum-nat was too fine and/or disordered to confirm its presence or detect any changes after activation. From previous studies, the role played by iron in alkali activation depends on the phase it is present in. Iron can be included within a geopolymer gel if it is available in solution during the polymerisation process, and hence in a reactive form, as shown for ferric nitrate solution and freshly precipitated ferric (oxy)hydroxide [70], as well as augite [71]. However, if the iron is held in an unreactive form, including ferran forsterite [71] or hematite [72], this iron does not participate, or can have a slight retardation effect. The effect of unreacted iron on strength is debated, with some studies suggesting it has little effect [24] and others suggesting it is deleterious [23]. Due to the complexity of these systems and the objectives, checking for elemental incorporation within the product phases is beyond the scope of this study. In summary, hematite did not prevent the formation of zeolitic phases in Bristol-nat and Bengaluru-nat, but the influence of the iron compound in the Khartoum-nat (likely goethite) may have contributed to a retarding effect on geopolymer formation. This is in broad agreement with previous studies.

Calcite is a common mineral in soils and many other deposits. Calcite is present in Bristol-nat and Khartoum-nat (Figure 4). Its main reflection at 29.4 °2θ is not reduced in either soil. This is in agreement with the dTG spectra, in which the calcite mass loss peak does not appreciably change after activation in both soils (Figure 14, Figure 16). Calcite can participate in dissolution and geopolymer formation to some extent, although reported effects on strength have been mixed [73, 74]. Ca^{2+} ions can fulfil the charge-balancing role in the aluminosilicate polymer framework [75], but the overall effect on alkali aluminosilicate phase formation depends on activating solution concentration [76], and quantity of soluble Ca in the system [77]. In this case it seems that the calcite underwent negligible dissolution, likely due to the presence of more reactive phases.

Organic matter in sub-soils is typically present as humus, a general term given to a variety of unidentifiable organic substances [29]. Organic compounds generally act as retardants in the setting of Portland cement [78], but their effect in alkali activation is not well-investigated so far. NaOH is commonly used to extract organic matter from soils undergoing testing [79]. The evidence so far suggests that adsorption onto mineral surface sites has an inhibiting effect for dissolution of both kaolinite [80] and smectite-illite [81], as well as binding free Ca

in solution [6]. However, as stated previously, soils with low organic content are used for stabilised soil materials, as this is a general requirement in earth building [30].

With regards to the associated minerals found in the synthetic soils, the coarse size of the added quartz (sieved to >63μm) made appreciable dissolution unlikely. Muscovite was generally observed to be unreactive. The exception was microcline, which consistently seemed to undergo a reduction in intensity, but only in the synthetic soils. With regards to the associated minerals found in the natural soils, quartz, microcline, albite, muscovite, chlorite, hornblende and calcite were likely to have made a negligible contribution, whilst the iron compounds hematite and siderite underwent an appreciable degree of dissolution.

4.4 Implications for practical adoption

As described in Section 1, a major barrier to adoption of these systems is a lack of understanding of which compositional factors are important in making a given soil well-suited for alkali activation, and which are not. The findings in this study have improved this understanding. Firstly, it has shown that clay mineralogy is the major determinant of which phase assemblages are formed. Secondly, that the associated minerals encountered in these soils do not increase the amount of product phase formed, but some iron compounds could have the potential to retard geopolymer formation. It is foreseen that this approach will develop into a process for identifying suitable soils – and the best way to activate them – by firstly investigating clay content and reactivity, and then assessing whether associated minerals are likely to be detrimental (e.g. possibly some iron compounds) or beneficial (e.g. reactive forms of silica).

In addition to the question of phase formation, another barrier that is often overlooked is achieving suitable workability. If a soil has a high plastic limit there is a trade-off between NaOH concentration and Na:Al molar ratio whilst maintaining mix workability at the plastic limit. As shown for Khartoum-nat, when a system molar ratio of Na:Al = 1 was used, the NaOH concentration was insufficient for a reaction to occur. When a 10 M NaOH solution was used, a product phase was formed but the Na:Al molar ratio far exceeded the ideal value of 1. This means there was an excess of Na in the system available to form soluble carbonates in the form of surface efflorescence, which poses practical difficulties in leaching and even potential for surface damage [82]. This study has shown that there is a trade-off in mix design between NaOH concentration and Na:Al molar ratio. As a result of this trade-off, although the mineralogy of montmorillonite-rich soils may be conducive to successful alkali activation, the practical production constraints make them unfeasible to use in their natural form using NaOH as the sole activator. However, there is still strong potential for alkali-activated soil systems, albeit using a range of activators, reactive precursors and/or

admixtures. The increased understanding of the fundamental behaviours developed in this study will assist the development of such systems.

4.5 Future research directions

This study has demonstrated the value of using synthetic soils to isolate the influence of different aspects of soil composition on alkali activation. There is potential to extend this approach in more detail to specific categories of associated minerals, particularly iron compounds, as these have the capacity to either contribute to or retard geopolymer formation. This further work will be needed in order to achieve the level of understanding required to assess whether, and how best, to use a soil for alkali activation. Moving beyond mineralogy, compressive strength testing under both dry and saturated conditions will be needed to link this new understanding of chemical phenomena in alkali activated soils to their mechanical properties. Finally, mix designs need to be developed which can balance the trade-off between system's Na:Al molar ratio, and the activator concentration. This understanding can underpin the future design and use of these materials in construction.

5 Conclusions

Clay minerals have been shown to be the primary determinants of phase formation in alkali-activated soils. In zeolite-forming soil systems, the scale and type of zeolite particles formed were influenced by clay particle size, mineralogy and possibly processing conditions. In contrast, through the innovative use of synthetic soil systems, it was shown that most associated minerals had little or no influence in the reaction. Regarding iron compounds, hematite did not prevent zeolite formation in two of the soil systems, but iron compounds may have had a retarding effect on geopolymer formation in the montmorillonite-rich soil. There is a trade-off in mix design between Na:Al molar ratio and NaOH concentration. Given this, in addition to clay mineralogy, it is the plastic limit which determines whether a given soil is suitable for alkali activation.

Acknowledgements

Thanks are given to Prof. BVV Reddy, Indian Institute of Science, and Dr. Amal Balila, University of Reading, for providing the Bengaluru and Khartoum soils respectively. Thanks are given to Ms. Preethi Krishnamurthy for providing additional information about the Bengaluru Soil. This study was supported by the EPSRC Centre for Decarbonisation of the Built Environment (dCarb) [grant number EP/L016869/1], a University of Bath Research Scholarship and the UKIERI project "Developing earth based building products utilising solid wastes". All data created during this research are openly available from the University of Bath data archive at https://doi.org/10.15125/BATH-00565.

References

[1] J.L. Provis, Alkali-activated materials, Cement and Concrete Research 114 (2018) 40-48. https://doi.org/10.1016/j.cemconres.2017.02.009

[2] P. Sargent, 21 - The development of alkali-activated mixtures for soil stabilisation, Handbook of Alkali-Activated Cements, Mortars and Concretes, Woodhead Publishing, Oxford, 2015, pp. 555-604.

[3] S. Pourakbar, B.K. Huat, A review of alternatives traditional cementitious binders for engineering improvement of soils, International Journal of Geotechnical Engineering 11(2) (2017) 206-216. https://doi.org/10.1080/19386362.2016.1207042

[4] H.N. Hamzah, M.M. Al Bakri Abdullah, H.C. Yong, M.R.R.A. Zainol, K. Hussin, Review of soil stabilization techniques: Geopolymerization method one of the new technique, Key Engineering Materials 660 (2015) 298-304. https://doi.org/10.4028/www.scientific.net/KEM.660.298

[5] N. Cristelo, S. Glendinning, L. Fernandes, A.T. Pinto, Effects of alkaline-activated fly ash and Portland cement on soft soil stabilisation, Acta Geotechnica 8(4) (2013) 395-405. https://doi.org/10.1007/s11440-012-0200-9

[6] K. Toda, H. Sato, N. Weerakoon, T. Otake, S. Nishimura, T. Sato, Key Factors Affecting Strength Development of Steel Slag-Dredged Soil Mixtures, Minerals 8(5) (2018) 174. https://doi.org/10.3390/min8050174

[7] B. Singhi, A.I. Laskar, M.A. Ahmed, Investigation on Soil–Geopolymer with Slag, Fly Ash and Their Blending, Arabian Journal for Science and Engineering 41(2) (2016) 393-400. https://doi.org/10.1007/s13369-015-1677-y

[8] J.M. Kinuthia, 9 - Unfired clay materials and construction, Nonconventional and Vernacular Construction Materials, Woodhead Publishing2016, pp. 251-272.

[9] A. Arulrajah, T.-A. Kua, C. Phetchuay, S. Horpibulsuk, F. Mahghoolpilehrood, M.M. Disfani, Spent Coffee Grounds-Fly Ash Geopolymer Used as an Embankment Structural Fill Material, Journal of Materials in Civil Engineering 28(5) (2016) 04015197. https://doi.org/10.1061/(ASCE)MT.1943-5533.0001496

[10] S. Pourakbar, A. Asadi, B.B.K. Huat, N. Cristelo, M.H. Fasihnikoutalab, Application of Alkali-Activated Agro-Waste Reinforced with Wollastonite Fibers in Soil Stabilization, Journal of Materials in Civil Engineering 29(2) (2017) 04016206. https://doi.org/10.1061/(ASCE)MT.1943-5533.0001735

[11] M. Zhang, H. Guo, T. El-Korchi, G.P. Zhang, M.J. Tao, Experimental feasibility study of geopolymer as the next-generation soil stabilizer, Construction and Building Materials 47 (2013) 1468-1478. https://doi.org/10.1016/j.conbuildmat.2013.06.017

[12] S. Omar Sore, A. Messan, E. Prud'homme, G. Escadeillas, F. Tsobnang, Stabilization of compressed earth blocks (CEBs) by geopolymer binder based on local materials from Burkina Faso, Construction and Building Materials 165 (2018) 333-345. https://doi.org/10.1016/j.conbuildmat.2018.01.051

[13] S. Miao, Z. Shen, X. Wang, F. Luo, X. Huang, C. Wei, Stabilization of Highly Expansive Black Cotton Soils by Means of Geopolymerization, Journal of Materials in Civil Engineering 29(10) (2017) 04017170. https://doi.org/10.1061/(ASCE)MT.1943-5533.0002023

[14] J. Dahmen, J. Kim, C.M. Ouellet-Plamondon, Life cycle assessment of emergent masonry blocks, Journal of Cleaner Production 171 (2018) 1622-1637. https://doi.org/10.1016/j.jclepro.2017.10.044

[15] J.L. Provis, Alkali-Activation of Calcined Clays – Past, Present and Future, in: F. Martirena, A. Favier, K. Scrivener (Eds.) Calcined Clays for Sustainable Concrete, Springer Netherlands, Dordrecht, 2018, pp. 372-376.

[16] A. McIntosh, S.E.M. Lawther, J. Kwasny, M.N. Soutsos, D. Cleland, S. Nanukuttan, Selection and characterisation of geological materials for use as geopolymer precursors, Advances in Applied Ceramics 114(7) (2015) 378-385. https://doi.org/10.1179/1743676115Y.0000000055

[17] A. Gharzouni, B. Samet, S. Baklouti, E. Joussein, S. Rossignol, Addition of low reactive clay into metakaolin-based geopolymer formulation: Synthesis, existence domains and properties, Powder Technology 288 (2016) 212-220. https://doi.org/10.1016/j.powtec.2015.11.012

[18] H. Rahier, B. Van Mele, M. Biesemans, J. Wastiels, X. Wu, Low-temperature synthesized aluminosilicate glasses. Part I Low-temperature reaction stoichiometry and structure of a model compound, J Mater Sci 31(1) (1996) 71-79. https://doi.org/10.1007/bf00355128

[19] J.G.S. van Jaarsveld, J.S.J. van Deventer, G.C. Lukey, The effect of composition and temperature on the properties of fly ash- and kaolinite-based geopolymers, Chemical Engineering Journal 89(1–3) (2002) 63-73. http://dx.doi.org/10.1016/S1385-8947(02)00025-6

[20] M.B. Diop, M.W. Grutzeck, Low temperature process to create brick, Construction and Building Materials 22(6) (2008) 1114-1121. http://dx.doi.org/10.1016/j.conbuildmat.2007.03.004

[21] M. Lassinantti Gualtieri, M. Romagnoli, S. Pollastri, A.F. Gualtieri, Inorganic polymers from laterite using activation with phosphoric acid and alkaline sodium silicate solution: Mechanical and microstructural properties, Cement and Concrete Research 67 (2015) 259-270. https://doi.org/10.1016/j.cemconres.2014.08.010

[22] C. Boutterin, J. Davidovits, Geopolymeric Cross-Linking (LTGS) and Building materials, Geopolymer ' 88, 1988.

[23] E. Obonyo, E. Kamseu, P. Lemougna, A. Tchamba, U. Melo, C. Leonelli, A Sustainable Approach for the Geopolymerization of Natural Iron-Rich Aluminosilicate Materials, Sustainability 6(9) (2014) 5535-5553. https://doi.org/10.3390/su6095535

[24] P.N. Lemougna, A.B. Madi, E. Kamseu, U.C. Melo, M.P. Delplancke, H. Rahier, Influence of the processing temperature on the compressive strength of Na activated lateritic soil for building applications, Construction and Building Materials 65 (2014) 60-66. https://doi.org/10.1016/j.conbuildmat.2014.04.100

[25] A. Marsh, A. Heath, P. Patureau, M. Evernden, P. Walker, Alkali activation behaviour of un-calcined montmorillonite and illite clay minerals, Applied Clay Science 166 (2018) 250-261. https://doi.org/10.1016/j.clay.2018.09.011

[26] F. Zibouche, H. Kerdjoudj, J.-B. d'Espinose de Lacaillerie, H. Van Damme, Geopolymers from Algerian metakaolin. Influence of secondary minerals, Applied Clay Science 43(3) (2009) 453-458. https://doi.org/10.1016/j.clay.2008.11.001

[27] S. Guggenheim, R. Martin, Definition of clay and clay mineral: Joint Report of the AIPEA and CMS Nomenclature Committees, Clay Miner 30(3) (1995) 257-259. https://doi.org/10.1180/claymin.1995.030.3.09

[28] F. Bergaya, G. Lagaly, Chapter 1 - General Introduction: Clays, Clay Minerals, and Clay Science, in: F. Bergaya, G. Lagaly (Eds.), Developments in Clay Science, Elsevier2013, pp. 1-19.

[29] J.B. Dixon, S.B. Weed, Minerals in Soil Environments, 2nd ed., Soil Science Society of America, Madison, WI, 1989.

[30] K. Jagadish, Building with Stabilized Mud, I.K. International Publishing House Pvt. Ltd., New Delhi, 2007.

[31] A. Marsh, A. Heath, P. Patureau, M. Evernden, P. Walker, A mild conditions synthesis route to produce hydrosodalite from kaolinite, compatible with extrusion processing, Microporous and Mesoporous Materials 264 (2018) 125-132. https://doi.org/10.1016/j.micromeso.2018.01.014

[32] A. Marsh, A. Heath, P. Patureau, M. Evernden, P. Walker, Phase formation behaviour in alkali activation of clay mixtures, Applied Clay Science 175 (2019) 10-21. https://doi.org/10.1016/j.clay.2019.03.037

[33] D. Maskell, Development of Stabilised Extruded Earth Masonry Units, Department of Architecture & Civil Engineering, University of Bath, 2013.

[34] A. Balila, Enhancing Strength and Durability of Adobe Bricks by Introducing Bio-inspired Stabilisers, School of the Built Environment, University of Reading, 2017.

[35] BSI, BS 1377-2:1990 Methods of test for soils for civil engineering purposes. Classification tests 1990.

[36] G. Habert, C. Ouellet-Plamondon, Recent update on the environmental impact of geopolymers, RILEM Technical Letters 1 (2016) 17-23. 10.21809/rilemtechlett.2016.6

[37] S. Hollanders, R. Adriaens, J. Skibsted, Ö. Cizer, J. Elsen, Pozzolanic reactivity of pure calcined clays, Applied Clay Science 132-133 (2016) 552-560. https://doi.org/10.1016/j.clay.2016.08.003

[38] S. Brunauer, P.H. Emmett, E. Teller, Adsorption of gases in multimolecular layers, Journal of the American chemical society 60(2) (1938) 309-319.

[39] J.F. Wagner, Chapter 9 - Mechanical Properties of Clays and Clay Minerals, in: F. Bergaya, G. Lagaly (Eds.), Handbook of Clay Science, Elsevier, Amsterdam, 2013, pp. 347-381.

[40] D.M. Moore, R.C. Reynolds, X-ray diffraction and the identification and analysis of clay minerals, 2nd ed., Oxford University Press, Oxford, 1997.

[41] J.W. Stucki, Chapter 11 - Properties and Behaviour of Iron in Clay Minerals, in: F. Bergaya, G. Lagaly (Eds.), Developments in Clay Science, Elsevier2013, pp. 559-611.

[42] J.W. Stucki, B.A. Goodman, U. Schwertmann, Iron in Soils and Clay Minerals Springer1987.

[43] R. Kuhnel, H. Roorda, J. Steensma, The crystallinity of minerals - a new variable in pedogenetic processes: a study of goethite and associated silicates in laterites, Clays and Clay Minerals 23(5) (1975) 349-354.

[44] R.C. Kaze, L.M. Beleuk à Moungam, M.L. Fonkwe Djouka, A. Nana, E. Kamseu, U.F. Chinje Melo, C. Leonelli, The corrosion of kaolinite by iron minerals and the effects on geopolymerization, Applied Clay Science 138 (2017) 48-62. https://doi.org/10.1016/j.clay.2016.12.040

[45] E. Ferrage, B. Lanson, B.A. Sakharov, V.A. Drits, Investigation of smectite hydration properties by modeling experimental X-ray diffraction patterns: Part I. Montmorillonite hydration properties, Am Mineral 90(8-9) (2005) 1358-1374. https://doi.org/10.2138/am.2005.1776

[46] J. Bain, A plasticity chart as an aid to the identification and assessment of industrial clays, Clay Miner 9(1) (1971) 1-17.

[47] E.C. Moloy, Q. Liu, A. Navrotsky, Formation and hydration enthalpies of the hydrosodalite family of materials, Microporous and Mesoporous Materials 88(1) (2006) 283-292. https://doi.org/10.1016/j.micromeso.2005.09.020

[48] A. Bauer, G. Berger, Kaolinite and smectite dissolution rate in high molar KOH solutions at 35° and 80°C, Applied Geochemistry 13(7) (1998) 905-916. http://dx.doi.org/10.1016/S0883-2927(98)00018-3

[49] S.J. Köhler, F. Dufaud, E.H. Oelkers, An experimental study of illite dissolution kinetics as a function of ph from 1.4 to 12.4 and temperature from 5 to 50°C, Geochimica et Cosmochimica Acta 67(19) (2003) 3583-3594. http://dx.doi.org/10.1016/S0016-7037(03)00163-7

[50] P.A. Jacobs, E.G. Derouane, J. Weitkamp, Evidence for X-ray-amorphous zeolites, Journal of the Chemical Society, Chemical Communications (12) (1981) 591-593. https://doi.org/10.1039/C39810000591

[51] W. Smykatz-Kloss, Differential Thermal Analysis: Application and Results in Mineralogy, Springer-Verlag Berlin Heidelberg Berlin; Heidelberg, 1974.

[52] A.L. Ulery, L.R. Drees, Methods of Soil Analysis Part 5—Mineralogical Methods, Soil Science Society of America, Madison, WI, 2008.

[53] V. Nikulshina, N. Ayesa, M.E. Gálvez, A. Steinfeld, Feasibility of Na-based thermochemical cycles for the capture of CO2 from air—Thermodynamic and thermogravimetric analyses, Chemical Engineering Journal 140(1) (2008) 62-70. https://doi.org/10.1016/j.cej.2007.09.007

[54] A. Newkirk, I. Aliferis, Drying and decomposition of sodium carbonate, Analytical Chemistry 30(5) (1958) 982-984.

[55] M. Földvári, Measurement of different water species in minerals by means of thermal derivatography, in: W. Smykatz-Kloss, S.S.J. Warne (Eds.), Thermal Analysis in the Geosciences, Springer Berlin Heidelberg, Berlin, Heidelberg, 1991, pp. 84-100.

[56] S.M. Rodulfo-Baechler, S.L. González-Cortés, J. Orozco, V. Sagredo, B. Fontal, A.J. Mora, G. Delgado, Characterization of modified iron catalysts by X-ray diffraction, infrared spectroscopy, magnetic susceptibility and thermogravimetric analysis, Materials Letters 58(20) (2004) 2447-2450. https://doi.org/10.1016/j.matlet.2004.02.032

[57] J.M. Criado, A. Ortega, A study of the influence of particle size on the thermal decomposition of CaCO3 by means of constant rate thermal analysis, Thermochimica Acta 195 (1992) 163-167. https://doi.org/10.1016/0040-6031(92)80059-6

[58] G. Engelhardt, J. Felsche, P. Sieger, The hydrosodalite system Na6+ x [SiAlO4] 6 (OH) x. cntdot. nH2O: formation, phase composition, and de-and rehydration studied by 1H, 23Na, and 29Si MAS-NMR spectroscopy in tandem with thermal analysis, x-ray diffraction, and IR spectroscopy, Journal of the American Chemical Society 114(4) (1992) 1173-1182. https://doi.org/10.1021/ja00030a008

[59] V. Drits, G. Besson, F. Muller, An improved model for structural transformation of heat-treated aluminous dioctahedral 2: 1 layer silicates, Clays and Clay Minerals 43(6) (1995) 718-731.

[60] F. Wolters, K. Emmerich, Thermal reactions of smectites—Relation of dehydroxylation temperature to octahedral structure, Thermochimica Acta 462(1) (2007) 80-88. https://doi.org/10.1016/j.tca.2007.06.002

[61] T. Abdullahi, Z. Harun, M.H.D. Othman, A review on sustainable synthesis of zeolite from kaolinite resources via hydrothermal process, Advanced Powder Technology 28(8) (2017) 1827-1840. https://doi.org/10.1016/j.apt.2017.04.028

[62] R. Barrer, J. Cole, H. Sticher, Chemistry of soil minerals. Part V. Low temperature hydrothermal transformations of kaolinite, Journal of the Chemical Society A: Inorganic, Physical, Theoretical (1968) 2475-2485. https://doi.org/10.1039/J19680002475

[63] G. Suraj, C.S.P. Iyer, S. Rugmini, M. Lalithambika, The effect of micronization on kaolinites and their sorption behaviour, Applied Clay Science 12(1) (1997) 111-130. https://doi.org/10.1016/S0169-1317(96)00044-0

[64] S. Lucas, M.T. Tognonvi, J.L. Gelet, J. Soro, S. Rossignol, Interactions between silica sand and sodium silicate solution during consolidation process, Journal of Non-Crystalline Solids 357(4) (2011) 1310-1318. https://doi.org/10.1016/j.jnoncrysol.2010.12.016

[65] H. Xu, J.S.J. Van Deventer, The geopolymerisation of alumino-silicate minerals, International Journal of Mineral Processing 59(3) (2000) 247-266. http://dx.doi.org/10.1016/S0301-7516(99)00074-5

[66] H. Xu, J.S.J. Van Deventer, Geopolymerisation of multiple minerals, Minerals Engineering 15(12) (2002) 1131-1139. https://doi.org/10.1016/S0892-6875(02)00255-8

[67] D. Feng, J.L. Provis, J.S.J. van Deventer, Thermal Activation of Albite for the Synthesis of One-Part Mix Geopolymers, Journal of the American Ceramic Society 95(2) (2012) 565-572. https://doi.org/10.1111/j.1551-2916.2011.04925.x

[68] L.T. Alexander, J.G. Cady, Genesis and hardening of laterite in soils, US Department of Agriculture, Washington, D.C. , 1962.

[69] K. Ishikawa, T. Yoshioka, T. Sato, A. Okuwaki, Solubility of hematite in LiOH, NaOH and KOH solutions, Hydrometallurgy 45(1) (1997) 129-135. https://doi.org/10.1016/S0304-386X(96)00068-0

[70] D.S. Perera, J.D. Cashion, M.G. Blackford, Z. Zhang, E.R. Vance, Fe speciation in geopolymers with Si/Al molar ratio of ~2, Journal of the European Ceramic Society 27(7) (2007) 2697-2703. https://doi.org/10.1016/j.jeurceramsoc.2006.10.006

[71] P.N. Lemougna, K.J.D. MacKenzie, G.N.L. Jameson, H. Rahier, U.F. Chinje Melo, The role of iron in the formation of inorganic polymers (geopolymers) from volcanic ash: a 57Fe Mössbauer spectroscopy study, J Mater Sci 48(15) (2013) 5280-5286. https://doi.org/10.1007/s10853-013-7319-4

[72] N. Essaidi, B. Samet, S. Baklouti, S. Rossignol, The role of hematite in aluminosilicate gels based on metakaolin, Ceramics Silikati 58(1) (2014) 1-11.

[73] C.K. Yip, J.L. Provis, G.C. Lukey, J.S.J. van Deventer, Carbonate mineral addition to metakaolin-based geopolymers, Cement and Concrete Composites 30(10) (2008) 979-985. https://doi.org/10.1016/j.cemconcomp.2008.07.004

[74] A. Cwirzen, J.L. Provis, V. Penttala, K. Habermehl-Cwirzen, The effect of limestone on sodium hydroxide-activated metakaolin-based geopolymers, Construction and Building Materials 66 (2014) 53-62. https://doi.org/10.1016/j.conbuildmat.2014.05.022

[75] I. Garcia-Lodeiro, A. Palomo, A. Fernández-Jiménez, 2 - An overview of the chemistry of alkali-activated cement-based binders, Handbook of Alkali-Activated Cements, Mortars and Concretes, Woodhead Publishing, Oxford, 2015, pp. 19-47.

[76] C.K. Yip, G.C. Lukey, J.S.J. van Deventer, The coexistence of geopolymeric gel and calcium silicate hydrate at the early stage of alkaline activation, Cement and Concrete Research 35(9) (2005) 1688-1697. https://doi.org/10.1016/j.cemconres.2004.10.042

[77] I. Garcia-Lodeiro, A. Palomo, A. Fernández-Jiménez, D.E. Macphee, Compatibility studies between N-A-S-H and C-A-S-H gels. Study in the ternary diagram Na2O–CaO–Al2O3–SiO2–H2O, Cement and Concrete Research 41(9) (2011) 923-931. https://doi.org/10.1016/j.cemconres.2011.05.006

[78] S. Paria, P.K. Yuet, Solidification–stabilization of organic and inorganic contaminants using portland cement: a literature review, Environmental Reviews 14(4) (2006) 217-255. https://doi.org/10.1139/a06-004

[79] M. Schnitzer, P. Schuppli, The extraction of organic matter from selected soils and particle size fractions with 0.5M NaOH and 0.1M Na4P2O7 solutions, Canadian Journal of Soil Science 69(2) (1989) 253-262. https://doi.org/10.4141/cjss89-026

[80] P.-K.F. Chin, G.L. Mills, Kinetics and mechanisms of kaolinite dissolution: effects of organic ligands, Chemical Geology 90(3) (1991) 307-317. https://doi.org/10.1016/0009-2541(91)90106-2

[81] F. Claret, A. Bauer, T. Schäfer, L. Griffault, B. Lanson, Experimental investigation of the interaction of clays with high-pH solutions: A case study from the Callovo-Oxfordian formation, Meuse-Haute Marne underground laboratory (France), Clays and Clay Minerals 50(5) (2002) 633-646. https://doi.org/10.1346/000986002320679369

[82] A. Allahverdi, E. Najafi Kani, K.M.A. Hossain, M. Lachemi, 17 - Methods to control efflorescence in alkali-activated cement-based materials, Handbook of Alkali-Activated Cements, Mortars and Concretes, Woodhead Publishing, Oxford, 2015, pp. 463-483.

Appendix

1 Introduction

As described in the Synthesis Procedure section in the main article, mix compositions were designed for efficient production of an alkali aluminosilicate phase and compatibility with extrusion processing. To this end, two constraints were used for each soil system: the wet mix had plastic limit consistency, and the system molar ratio Na:Al = 1. Given the differences in plastic limit between the soils (Figure 2 in the main article), the NaOH solution had a lower concentration for Khartoum (4.1 M) than for Bristol (13.2 M) and Bengaluru (10.2 M) (Table 3 in the main article). After activation, it was observed that new microstructural features had formed in Khartoum-syn, believed to be a N-A-S-H or (N,C)-A-S-H geopolymer phase. In contrast, in Khartoum-nat there was no evidence of new phase formation, with clay particles showing evidence of only partial dissolution at their edges (Section 3.2.3 in the main article).

To test whether associated minerals were preventing the formation of a geopolymer phase, or just retarding it, activation of the Khartoum soils was repeated using a 10 M NaOH activating solution. This concentration was chosen as it is a similar value to those in the other soil systems, and because the optimal concentration range for alkali activation of uncalcined clays using NaOH solution is understood to be in the range of 8 – 12 M [1-5]. New mix compositions were designed to maintain the plastic limit condition whilst using a 10 M concentration. This broke the second constraint, giving a system Na:Al molar ratio greater than 1. These additional results are presented here, with attention given to the phase formation in the additional systems, and comparison between the 10 M and 4.1 M systems for both Khartoum-nat and Khartoum-syn.

2 Materials and Methods

The same precursors were used as described in the main article, using a soil mass of 20 g for each mix. The activating solution quantities are given in *Table A6*. These quantities gave a Na:Al molar ratio of 2.4 in the activated systems.

Table A6: Composition of activating solutions used for 20g of dry soil.

Sample	Water (g)	NaOH (g)	[NaOH] molarity
Khartoum-nat-act10M	5.1	2.2	10.0
Khartoum-nat-act	5.5	0.9	4.1
Khartoum-syn-act10M	5.1	2.2	10.0
Khartoum-syn-act	5.5	0.9	4.1

The same preparation procedures and characterisation methods were used as described in the main article.

3 Results

3.1 Macroscopic behaviour

There were no major changes in form or appearance between the 10 M and original 4.1 M activated samples of either natural or synthetic Khartoum soils (*Figure A17*). There was slightly more colour contrast between the top and rest of the cylinders for the 10 M samples, again likely to be associated with the one-dimensional flow of soluble matter to the top of the sample, since a mould with one open end was used. Unlike for the original 4.1 M samples, no major cracks developed in demoulding the 10 M activated cylinders, indicating potentially improved binding.

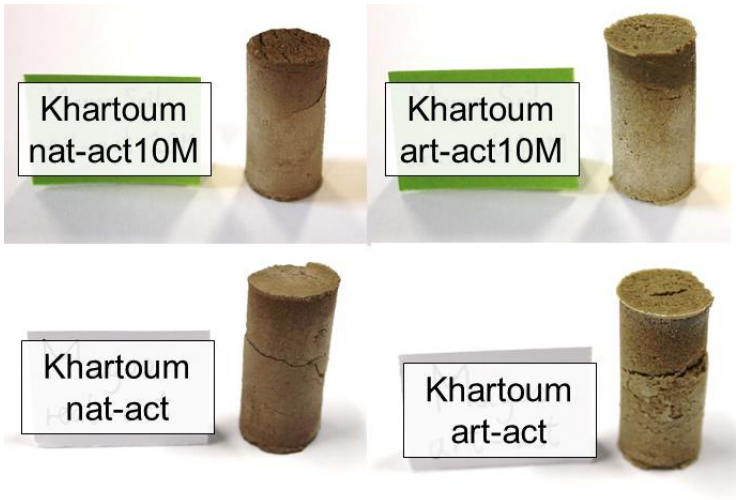

Figure A17: Photos of the 10 M and original 4.1 M activated samples of the natural and synthetic Khartoum soils.

3.2 XRD

In the 10 M activated samples new reflections emerged, attributed to a small amount of hydrosodalite phase (*Figure A18*). Given the small number of clearly visible reflections, it was not possible to index this with complete confidence, but was attributed to the non-basic hydrosodalite $Na_6[AlSiO_4]_6 \cdot 4H_2O$ (PDF# 00-042-0216). This was accompanied by a large reduction in intensity of the kaolinite reflections. With regards to the associated minerals, no large changes were observed relative to the original 4.1 M activated samples. The only small difference of note was the variability of the intensity of the microcline reflections at 27.5 °2θ, which suggests this may have been more to do with orientation than consumption. In Khartoum-nat, there was a decrease in intensity of the calcite peak at 29.4 °2θ.

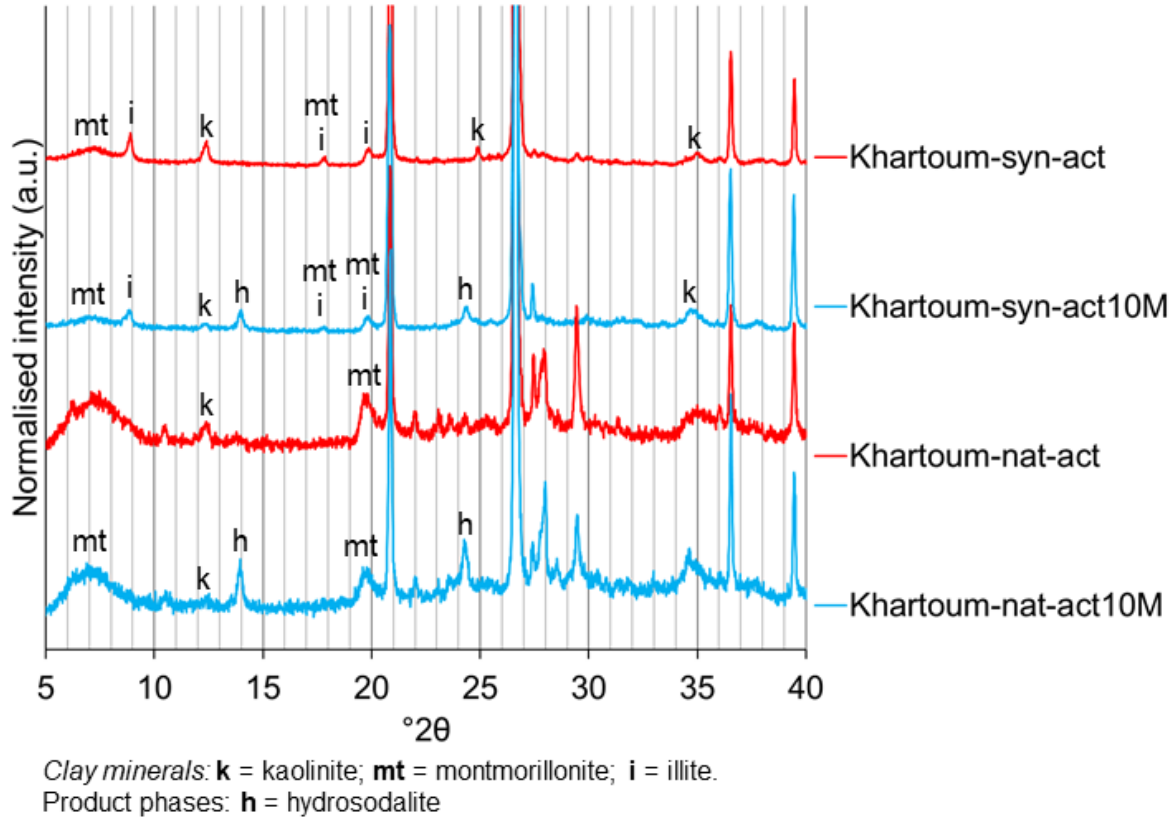

Figure A18: XRD patterns of the 10 M and original activated samples of the natural and synthetic Khartoum soils.

3.3 SEM

In the 10 M activated sample of Khartoum-nat (*Figure A19*), the same ragged clay particles were present as with the original 4.1 M activated sample – however, new particles also appeared to be present, of particle size <500 µm. In the 10 M activated sample of Khartoum-syn (*Figure A19*), the microstructure was dominated by irregular particles, which seemed to be more connected and with a wider size distribution than in the original 4.1 M activated synthetic sample.

In both the natural and synthetic soils, there seemed to be changes in the SEM images for the 10 M activated sample relative to the original 4.1 M activated sample, although some overall similarities in microstructure were maintained.

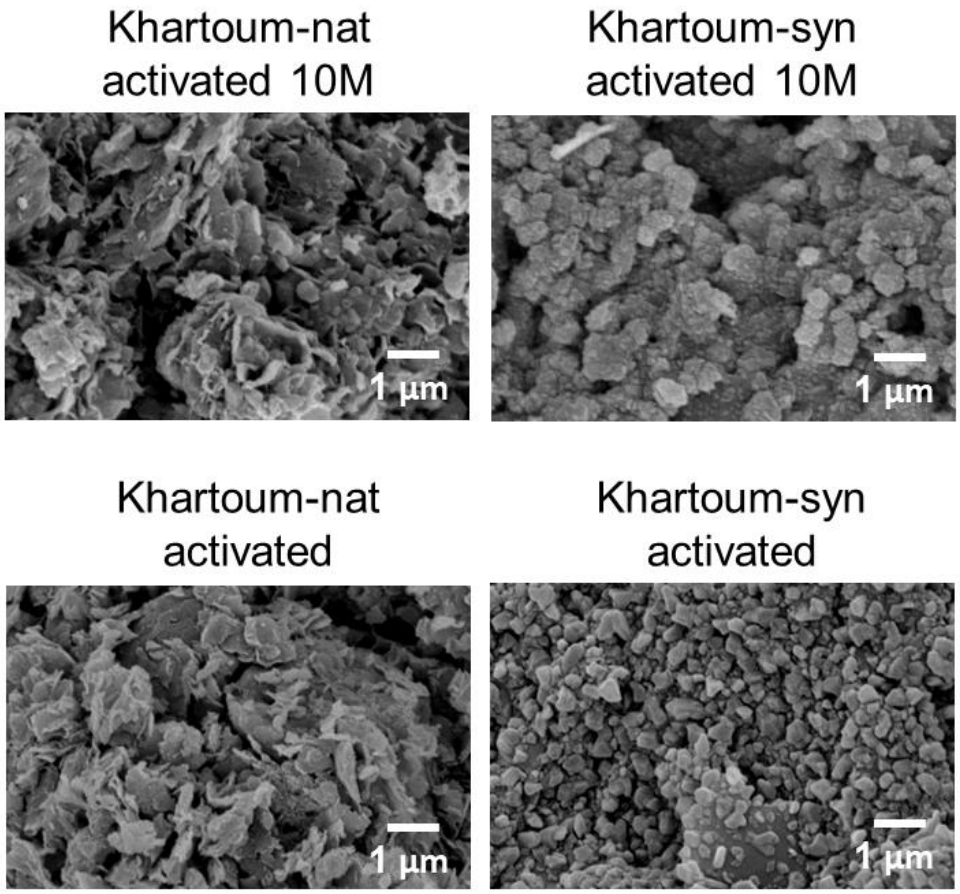

Figure A19: SEM images of the 10 M and original activated samples of the natural and synthetic Khartoum soils.

3.4 FTIR

Some similar changes were observed for both natural and synthetic soils for 10 M activation relative to the original 4.1 M activation (*Figure A20*). In Khartoum-syn, the 10 M NaOH activation led to a small positive shift in wavenumber of the Si-O-T band peak, from 1031 to 1035 cm^{-1}. However, the profile of this band clearly changed with a more prominent shoulder on the lower wavenumber side. In Khartoum-nat, there was a negative shift in wavenumber of the Si-O-T band peak, from 1004 to 988 cm^{-1}. This was especially striking, since the wavenumber position in the precursor was 1003 cm^{-1}. This suggested that an alkali aluminosilicate product had formed after 10 M activation, but not after the original 4.1 M activation.

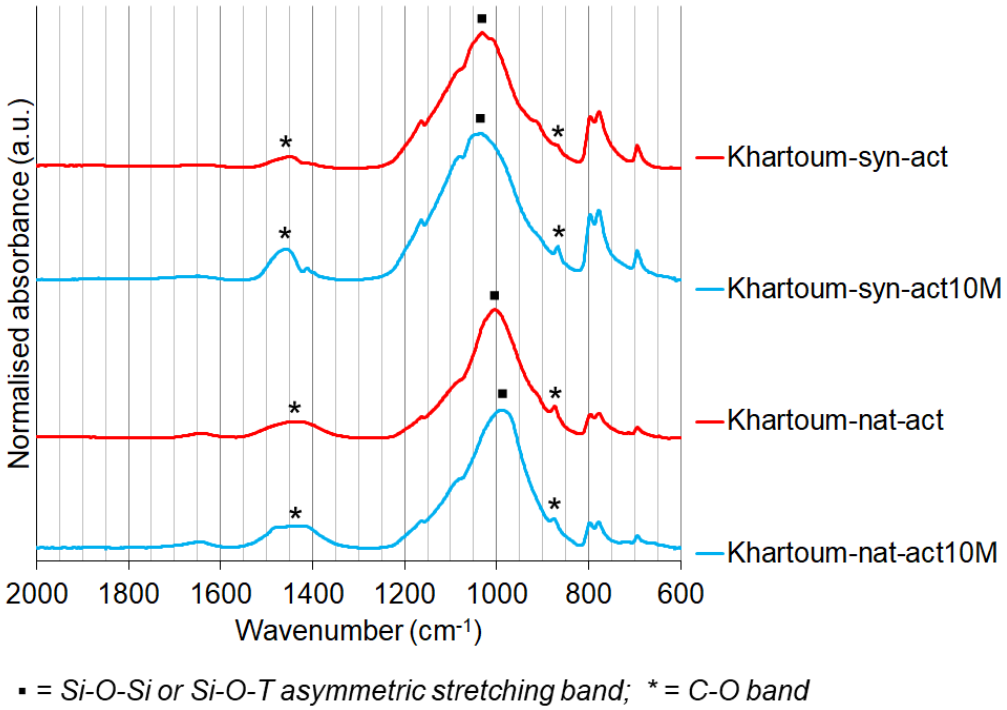

Figure A20: FTIR spectra of the 10 M and original activated samples of the natural and synthetic Khartoum soils.

3.5 TGA

In the TGA and dTG spectra (*Figure A21*), the same features were present in the 10 M and original 4.1 M activated samples, but these were more pronounced in the 10 M samples. Several changes were common to both soils with the increase to 10 M. Overall mass loss increased by 3.0% for both. There was an increase in the surface-adsorbed moisture dTG peak (centre at 83 °C), and an increase in the background signal to form a plateau between 150 - 350 °C, which is associated with geopolymer formation [6]. This was in agreement with

the FTIR results, which suggested a geopolymer phase had formed in Khartoum-syn-act10M.

Regarding clay minerals, no large changes were visible for Khartoum-syn-act10M. In Khartoum-nat-act10M there was overlap with the positions of the dTG peaks and the plateau region between 150-350 °C. Regarding associated minerals, there was a noticeable decrease in intensity of the calcite dTG peak (centre at 661 °C) for Khartoum-nat, in agreement with the XRD observations.

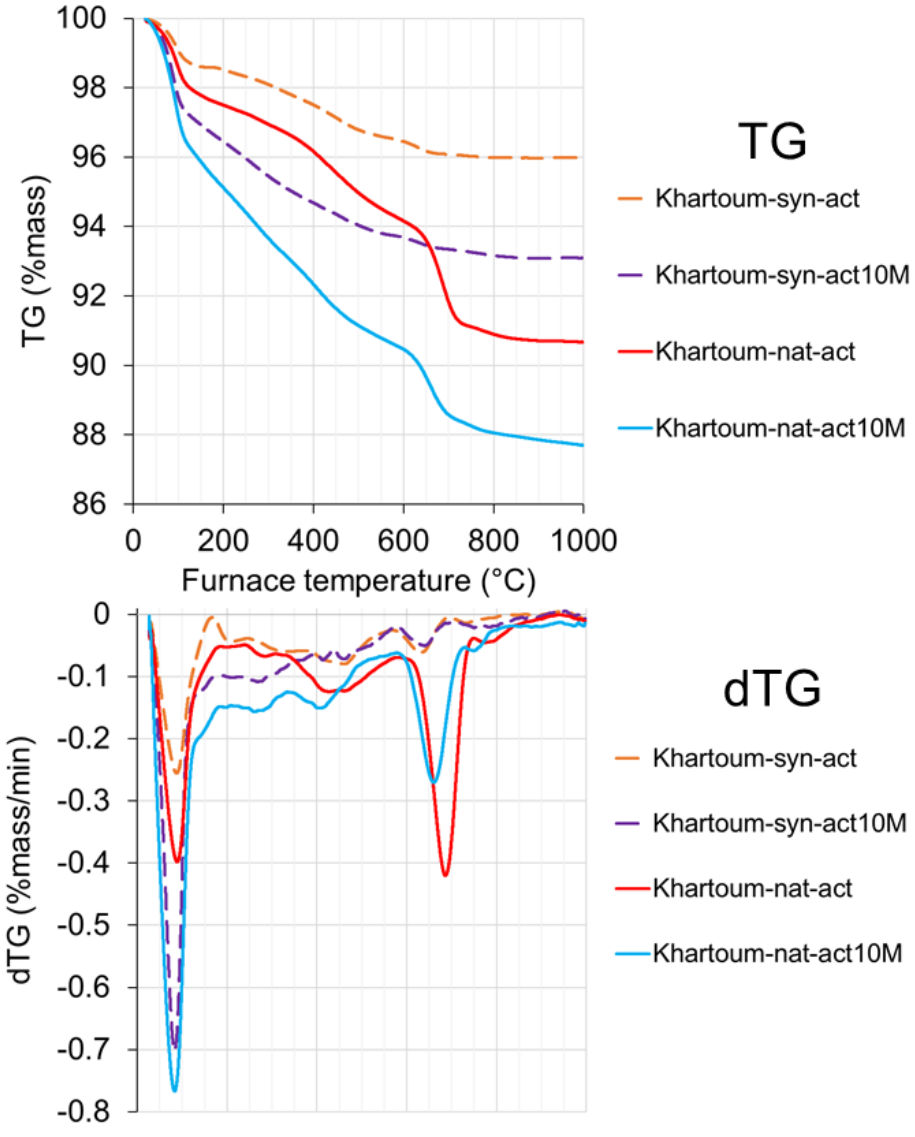

Figure A21: TG and dTG spectra of the 10 M and original activated samples of the natural and synthetic Khartoum soils.

4 Discussion

Apart from the fact that kaolinite was consumed in the 10 M activated samples (and was not in the original 4.1 M activated samples), behaviour of the clay minerals was largely the same in the 10 M and original activated samples. Regarding the associated minerals, this was also largely the same, with the exception of some degree of calcite consumption in Khartoum-syn as described in the XRD and TGA results. The discussion will then focus on the kaolinite and phase formation behaviour.

When 10 M activation was used, kaolinite was consumed and hydrosodalite formed in both the natural and synthetic soils. This was not observed for the original 4.1 M activated samples. Both soils contained just 4 wt.% kaolinite, and the XRD patterns showed that not all kaolinite was consumed (*Figure A18*). Therefore it seems likely that the changes observed in the different characterisation techniques were not wholly due to hydrosodalite formation, and that geopolymer formation also occurred in both soils, but this is more difficult to quantitatively identify. As mentioned in the main article, a useful comparison system is from a study on the activation of controlled mixtures of clays under the same processing conditions [7]. The clay mineral composition of the Khartoum soil falls between those of the systems 90%Mont-10%Kao, 50%Mont-50%Kao and 33%Kao-33%Mont-33%ILL. From these compositions, at comparable NaOH concentrations, both a geopolymer and a hydrosodalite would be expected to form. The participation of kaolinite only at higher concentration is also in agreement with the cited study which suggested that montmorillonite reacts preferentially to kaolinite under these processing conditions [7]. Whereas in the original activated samples only a geopolymer was formed for Khartoum-syn, in the 10 M activated samples both a geopolymer and a hydrosodalite formed in Khartoum-nat and Khartoum-syn. This therefore suggests that whilst the associated minerals in Khartoum-nat may have prevented geopolymer formation at 4.1 M, a geopolymer was successfully formed at 10 M, meaning that the associated minerals in Khartoum-nat may have a retarding rather than a preventative effect on geopolymer formation.

5 Conclusions

These results show evidence for geopolymer and hydrosodalite formation in both natural and synthetic soils using 10 M NaOH. This suggests that in the lower concentration activation of the natural soil, geopolymer formation was retarded, but not prevented, relative to the synthetic soil.

References

[1] M.B. Diop, M.W. Grutzeck, Low temperature process to create brick, Construction and Building Materials 22(6) (2008) 1114-1121 http://dx.doi.org/10.1016/j.conbuildmat.2007.03.004

[2] P.N. Lemougna, A.B. Madi, E. Kamseu, U.C. Melo, M.P. Delplancke, H. Rahier, Influence of the processing temperature on the compressive strength of Na activated lateritic soil for building applications, Construction and Building Materials 65 (2014) 60-66 https://doi.org/10.1016/j.conbuildmat.2014.04.100

[3] H. Xu, J.S.J. Van Deventer, The geopolymerisation of alumino-silicate minerals, International Journal of Mineral Processing 59(3) (2000) 247-266 http://dx.doi.org/10.1016/S0301-7516(99)00074-5

[4] C.Y. Heah, H. Kamarudin, A.M. Mustafa Al Bakri, M. Bnhussain, M. Luqman, I. Khairul Nizar, C.M. Ruzaidi, Y.M. Liew, Kaolin-based geopolymers with various NaOH concentrations, Int J Miner Metall Mater 20(3) (2013) 313-322 https://doi.org/10.1007/s12613-013-0729-0

[5] A.D. Hounsi, G. Lecomte-Nana, G. Djétéli, P. Blanchart, D. Alowanou, P. Kpelou, K. Napo, G. Tchangbédji, M. Praisler, How does Na, K alkali metal concentration change the early age structural characteristic of kaolin-based geopolymers, Ceramics International 40(7, Part A) (2014) 8953-8962 http://dx.doi.org/10.1016/j.ceramint.2014.02.052

[6] A. Marsh, A. Heath, P. Patureau, M. Evernden, P. Walker, Alkali activation behaviour of un-calcined montmorillonite and illite clay minerals, Applied Clay Science 166 (2018) 250-261 https://doi.org/10.1016/j.clay.2018.09.011

[7] A. Marsh, A. Heath, P. Patureau, M. Evernden, P. Walker, Phase formation behaviour in alkali activation of clay mixtures, Applied Clay Science 175 (2019) 10-21 https://doi.org/10.1016/j.clay.2019.03.037